Supplementary Information

Benchmark uranium extraction from seawater by an ionic macroporous MOF

Samraj Mollick,[a] Satyam Saurabh,[a†] Yogeshwar D. More,[a†] Sahel Fajal,[a] Mandar M. Shirolkar,[b] Writakshi Mandal,[a] Sujit K. Ghosh[a,c*]

[a]Department of Chemistry, Indian Institute of Science Education and Research (IISER), Dr. Homi Bhabha Road, Pashan, Pune 411008, India.

[b]Symbiosis Center for Nanoscience and Nanotechnology (SCNN), Symbiosis International (Deemed University) (SIU), Lavale, Pune 412115, India.

[c]Centre for Water Research (CWR), IISER Pune.

[†]S. S. and Y.D.M. contributed equally to this work.

Corresponding author. E-mail: sghosh@iiserpune.ac.in

Table of Contents

Materials	S-3
Materials synthesis	S-3 to S-4
Characterization and physical measurements	S-4 to S-5
Capture study	S-5 to S-9
Structure simulation studies	S10
Characterization of materials	S-11 to S-20
Analysis of capture studies	S-21 to S-38
Breakthrough setup	S-39
Comparison with other works	S-42 to S-42
Post capture analysis	S-43 to S-51
Theoretical studies	S-52 to S-56
References	S-57

Materials

ZIF-90 was synthesized by the previously reported literature method.[1] All the reagents and solvents were commercially available and used as received. All the commercially available materials were bought from Sigma-Aldrich, TCI Chemicals, Avra Chemicals, and Alfa aesar depending on their availability.

Methods

Materials Synthesis

Synthesis of Nanosized UiO-66-NH_2. The nanosized UiO-66-NH_2 were synthesized according to the literature reported protocol.[2] 2-aminoterephthalic acid (668 mg, 3.69 mmol) and $ZrCl_4$ (233 mg, 1 mmol) were mixed in 60 mL DMF in a tightly capped glass jar and ultrasonicated for 15 min. Next, 4.5 mL acetic acid was added to the container and heated at 120 °C for 8 h. The mixture was cooled down to room temperature and yellow powder was collected by centrifugation and washed with DMF and hot ethanol and further dried under vacuum at 60 °C for 8 h.

Synthesis of IB@UiO-66-NH_2. The pristine nanosized UiO-66-NH_2 (500 mg, 1.97 mmol) and 2-Imidazolecarboxaldehyde (IB) (576.5 mg, 6 mmol) were suspended in ethanol solution and refluxed at 100 °C for 24 h. Afterwards, the solid was filtered and washed with fresh ethanol (50 mL) four times and dried under vacuum at 60 °C for overnight.

Synthesis of hybrid UiO-66-NH_2@ZIF-90. First, 20 mg of IB@UiO-66-NH_2, 384 mg (4 mmol) 2-Imidazolecarboxaldehyde (IB) and 296 mg (1 mmol) of zinc nitrate hexahydrate were mixed in 10 mL of methanol and finely dispersed by ultrasonication for 10 min. Next, 560 μL (4 mmol) triethyl amine base was added to the solution mixture and stirred for the next 24 h. Finally, the solid was collected by centrifugation and washed with a copious amount of hot DMF and methanol. After washing, the collected powder was dried under vacuum at 60 °C for 12 h. Various UiO-66-NH_2@ZIF-90 composites were also prepared following the aforementioned method where the amount of IB@UiO-66-NH_2 gradually increased from 10 to 20 to 40 to 50 to 100 to 200 mg and keeping the fixed amount of ZIF-90 components; the resultant materials are denoted as i-MZIF90(10), i-MZIF90(20), i-MZIF90(40), i-MZIF90(50), i-MZIF90(100) and i-MZIF90(200) respectively. Additionally, we have also synthesized nonhybridized composite material (UiO-66@ZIF-90) using UiO-66 MOF instead of IB@UiO-66-NH_2. The amount of MOF was used here 50 mg while keeping the 2-Imidazolecarboxaldehyde (IB: 4 mmol) and zinc nitrate hexahydrate (1 mmol) remains constant.

Synthesis of functionalized macroporous i-MZIF90. The different hybrid UiO-66-NH_2@ZIF-90 were dispersed in 5 mL of KOH solution (pH~12) and stirring continued for 72 h. The base solution was replaced by freshly prepared solutions two times a day. During this base treatment, the edx analysis of the materials was carried out after a certain time interval. The Zr contents gradually decrease with increasing the base treatment time and most of the Zr were leach out after 72 h.

Characterizations and physical measurements

Powder X-ray diff reaction (PXRD) patterns were performed on a Bruker D8 Advanced X-ray diffractometer at room temperature using Cu Kα radiation (λ = 1.5406 Å) at a scan speed of 0.5 ° min^{-1} and a step size of 0.01° in 2θ. Thermogravimetric analysis profiles were recorded on Perkin-Elmer STA6000, TGA analyser under N_2 atmosphere with heating rate of 10° C min^{-1}. The morphology of the crystalline materials was recorded with a Zeiss Ultra Plus field-emission scanning electron microscope (FESEM) with an integral charge compensator and embedded EsB

and AsB detectors (Oxford X-max instruments 80 mm^2 (Carl Zeiss NTS, GmbH). The samples were sputter-coated with a 5-10 nm Au film to reduce charging. The elemental analysis was carried out using voltage of 15 KV equipped with an EDX detector. Data acquisition was performed with an accumulation time of 600s. For high-resolution TEM analysis, all the samples were dispersed in isopropanol (0.5 mg/mL) and sonicated for 30 min. Then, the samples were left for 2 min, and the upper part of the solution was taken for preparing TEM samples on a lacey carbon-coated copper grid (Electron Microscopy Science). TEM imaging was performed on the HRTEM (JEM-2200FS, JEOL) operating at acceleration voltage of 200 kV. ^{13}C solid state NMR spectra were recorded on Bruker 400 MHz NMR spectrometer. Carbon chemical shifts are expressed in parts per million (δ scale). The IR Spectra were acquired by using NICOLET 6700 FT-IR spectrophotometer using KBr pellet in 500-4000 cm^{-1} range. Gas adsorption measurements were performed using BelSorp-Max instrument (Bel Japan). Prior to adsorption measurements, the activated samples were heated at 120 °C under vacuum for 12 h using BelPrepvacII. The fluorescence imaging was recorded on Leica DM6B EPI-Fluorescence instrument. ICP-AES analysis were performed on ARCOS, Simultaneous ICP Spectrometer. ICP-MS was performed on Quadrupole inductively coupled plasma mass spectrometry (Thermo Fisher Scientific) instrument. Multielement standards were purchased from inorganic ventures. XPS studies was performed using K-Alpha+model (Thermo Fischer Scientific, UK) with Al Kα source.

Capture Study

Adsorption study. U(VI) solution was prepared by dissolving uranyl nitrate hexahidrate ($UO_2(NO_3)_2.6H_2O$) salts in deionised water. The pH value adjusted by KOH (1M) solution.

In kinetics experiments, the U solution with initial concentration of 50 ppm. The adsorbent was 20 mg while the U solution was 35 mL. The adsorbent was well-dispersed by sonication, and afterwards the mixture was vigorously stirred during the kinetics experiments. At appropriate time intervals, aliquots (3 mL) were taken from the mixture and the adsorbents were filtered with a 0.22 μm nylon membrane filter and analyzed by using ICP-MS to determine the UO_2^{2+} content.

From this time dependent study we calculated the removal % and decreasing concentration of the U with time using the following equations: $D_t = [(C_0-C_t)/C_0]*100$; Where, D_t = exchange capacity, C_0= initial concentration, C_t= final concentration at specific time. The adsorption kinetics was analyzed by simplified kinetic models such as the pseudo-first-order and pseudo-second-order, through the following two equations,

$$\ln(Q_e-Q_t) = \ln Q_e - k_1$$

Where, Q_e and Q_t are the amount of U ion adsorbed at equilibrium and time t, t is adsorption time, and K_1 is the pseudo-first order constant of adsorption.

$$t/Q_t = 1/(k_2* Q_e) + (t/Q_e)$$

Where, Q_e and Q_t are the amounts of U ion capacity corresponding to different equilibrium and time respectively, t is adsorption time, and K_2 is the pseudo-second order constant of adsorption.

In isotherm experiments, the U solution with initial concentration 25-1000 ppm and the pH~7 was used. The aqueous solutions of uranium with different concentrations were obtained by diluting the stock U solution with the proper amount of distilled water unless otherwise indicated. The adsorbent was 2 mg while the U solution was 4 mL and the contact time is 12 h. The adsorbents were well-dispersed by brief sonication and then the mixtures were vigorously stirred throughout the experiments. The filtrate were collected through 0.2 μm syringe filter after 12 h and measured the concentration through ICP-AES and further fitted with following equations,

Langmuir Model, $Q_e = (Q_m*C_e)/(K_L+C_e)$; Where, C_e(ppm) and Q_e(mg g^{-1}) are the U concentration at equilibrium and amount of U adsorbed at equilibrium respectively. Q_m (mg g^{-1}) is the maximum amount of U per mass of adsorbent to form a complete monolayer. K_L (mg L^{-1}) is a constant related to the binding strength.

Freundlich Model, $Q_e = K_f*(Ce)1^{/n}$; Where, K_f and 1/n are the Freundlich model constant, indicating capacity and intensity of adsorption respectively.

In pH dependent study, the U solution with pH ~7 to 12 was adjusted by adding KOH (1 M). The adsorbent was 2 mg while the U solution was 4 mL and the contact time is 12 h. The adsorbents were well-dispersed by brief sonication and the mixtures were vigorously stirred throughout the experiments. The filtrate was collected through a 0.2 μm syringe filter after 12 h and measured the concentration through ICP-AES.

Capture study of U in presence of other competing ions. For testing the influence of competing ions, equimolar as well as a mixture of competing salts (KCl, NaCl, $CaCl_2$, $Mg(NO_3)_2$, $SrCl_2$, $CdCl_2$) were added to the U solution and carried out the capture studies. In these selective adsorption experiments, the adsorbent was 2 mg while the U spiked water was 2 mL with an initial concentration of 5 ppm and a contact time is 2 h. The solution mixtures were vigorously stirred throughout the experiments. The filtrate was collected through a 0.2 μm syringe filter after 12 h and measured the concentration through ICP-MS.

The K_d value and the selectivity (S) are calculated from the following two equations,

$$K_d = [(C_0-C_e)/C_e).(V/m).10^3]$$

$$S = K_d^U/K_d^M$$

where the unit for K_d value is mL/g, V is the volume of the treated solution (mL), m is the amount of adsorbent (mg), C_0 is the initial concentration of uranium, and C_e is the equilibrium concentration of uranium.

Validation of U capacity from spiked seawater and DI water. For spiked seawater experiments, the adsorbent was 10 mg while the U spiked seawater was 100 mL with an initial concentration of 100 ppm and the contact time is 12 h. For DI water experiments, the adsorbent was 10 mg while the U spiked seawater was 100 mL with an initial concentration of 200 ppm and the contact time is 12 h. The adsorbent was collected after isotherm experiments in spiked seawater by centrifugation and the filtrate was collected for the analysis. The collected adsorbent was digested with six molar nitric acids and further analysed the uranium content from the digested samples. The uranium adsorption capacity measured from the concentration of the solution and by the digestion process is compared for the validation of the U capacity from seawater.

Capacity of other metal ions including U from spiked seawater. In these experiments, the adsorbent was 5 mg while the U spiked seawater was 100 mL with an initial concentration of different metal ions were 50 ppm and a contact time is 12 h. Here, vanadium, iron, zinc, lead, nickel and copper metal salts were used as the source of other metal ions along with U(VI) salt. The adsorbents were well-dispersed by brief sonication and then the mixtures were vigorously stirred throughout the experiments. The filtrate was collected through a 0.2 μm syringe filter after 12 h and analyzed the metal ions concentration using ICP-AES.

Trace amount U capture studies. Trace amount of uranium capture studies performed for artificial seawater. A wide range of concentrations such as 5000 ppb, 1000 ppb, 500 ppb, 100 ppb, 50 ppb and 10 ppb of U capture studies were performed in a 15 mL drum vial equipped with magnetic stir bars at ambient temperature with a constant stirring rate of 400 r.p.m. 5 mg of i-MZIF90(50) was taken in a 5 mL of U containing solution. The mixtures were stirred at room temperature for 2h, filtered through a 0.22 μm membrane filter, and the filtrate was collected and analyzed by using ICP-MS to determine the remaining UO_2^{2+} content.

U removal kinetics from various water samples (potable water, lake water, river water, artificial seawater). The simulated seawater was prepared by following the literature report published elsewhere.[3] U spiked various water samples (5 ppm, 35 mL) and adsorbents (10 mg) were added to a 50 mL conical with a magnetic stir bar and the mixture was vigorously stirred at room temperature. At appropriate time intervals, aliquots (5 mL) were taken from the mixture and the adsorbents were filtered with a 0.22 μm nylon membrane filter. The U concentrations in the resulting solutions were analyzed by ICP-MS.

U removal kinetics from seawater. For testing the U removal kinetics from nonspkied natural seawater, 10 mg of adsorbents were added to 35 mL of seawater sample. The adsorbent was well-dispersed in seawater by sonication for 5 minutes and afterwards, the mixture was vigorously stirred during the kinetics experiments. At appropriate time intervals, aliquots (5 mL) were taken from the mixture and the adsorbents were filtered by a syringe filtered with a 0.22 μm membrane filter. The U concentrations in the resulting solutions were analyzed by ICP-MS.

Recyclability test from spiked water. U loaded material was regenerated in presence of 0.1 M K_2CO_3 solution, where loaded materials were stirred for ~ 10 h. Next, the absorbent was

collected by centrifugation and washed thrice with a copious amount of DI water and once with excess methanol. Afterwards, the adsorbent was dried under a vacuum at 65 °C, and again the i-MZIF90(50) was utilized for the next cycle.

Recyclability test from spiked seawater. For this test, 50 mg of i-MZIF90(50) was used as adsorbents while the U spiked seawater was 100 mL with an initial concentration of 100 ppm and the contact time is 12 h. After adsorption studies, the adsorbent was collected by centrifugation and the filtrate was collected for analysis. Next, the U-loaded material was regenerated presence of 0.1 M K_2CO_3 solution, where loaded materials were stirred for the next ~ 10 h. Afterwards, the absorbent was collected by centrifugation and washed thrice with a copious amount of DI water and once with excess methanol. Finally, the adsorbent was dried under a vacuum at 65 °C, and again the i-MZIF90(50) was utilized for the next two cycles.

U uptake via breakthrough experiments. ~ 1 g of i-MZIF90(50) and 25 g of sand were mixed in a mortar pestle and filled in a glass tube with an inner aperture of 6 mm and a length of 2.5 ft. To minimize the leaching possibility of the material, little amount of cotton was kept at the bottom of the composite and sand mixture. The solution contained U and other salts KCl, NaCl, $CaCl_2$, $Mg(NO_3)_2$, $SrCl_2$, $CdCl_2$ and their initial concentration was kept ~ 3 ppm. Prior to the breakthrough experiment, the column was washed with excess water and the flow rate was fixed to 0.12 mL/min for the outflow solution. The collected filtrate was analyzed the metal ions concentration using ICP-AES. The schematic diagrams of the breakthrough setup was provided in Figure S32.

U extraction from Seawater. We have collected 180 L of seawater from the Arabian sea (Juhu beach, Mumbai, India) for extraction of U from seawater. We have carried out the seawater experiments for three different batches (60 L in each batch) at room temperature and 4.8 mg of i-MZIF90(50) was used as an adsorbent in each experiment. Samples were first sonicated in 50 mL seawater for 5 minutes prior to mixing in 60 L seawater. We mixed the whole seawater solution 5 times a day with a long stick and each time we stirred for ~ 2 minutes on regular basis. At appropriate time intervals, 15 mL aliquots were taken out from the mixture and the adsorbents were filtered with a 0.2 μm syringe filter. Finally, the adsorption of U was analyzed through ICP-MS.

Structure simulation studies

Materials Studio software suite 2017 (Accelrys) was used to perform the structural simulation studies. Initially, the molecular structure of the single MOF unit cell was fully relaxed using DMOL3 code and B3LYP hybrid exchange correlation function. The multiplicity factor was kept to Auto mode and Double Numeric Plus Polarizing (DNP+) as Basis set and water as solvent was considered for the simulations. The structural simulation was performed with medium quality Global orbital cutoff scheme. For the geometry relaxation of the MOF unit cell, energy, force and displacement parameters were set to 2 × 10-5 Ha, 0.004 Ha/Å and 0.005 Å respectively. On this geometry relaxed MOF unit cell the structural simulation was performed using a Universal force field at fine quality calculation level. The Connolly surface was constructed using Atom, Volumes and Surface tools available in Materials Studio, with a fine grid resolution of 0.25 Å with Connolly radius of 1.0 Å. Using the Sorption module, the possible interaction sites of different guest molecules introduced in the MOF unit cell were modelled. The calculations were performed using the Metropolis algorithm with fine quality grid calculations at a temperature of 298 K on a single MOF unit cell and 3×3×3 supercell.

Determination of binding energy of interactions, electrostatic-potential surface (ESP) and binding sites

Using Discovery Studio 2016 (Accelrys) we obtained interactions between MOF unit and guest molecules in terms of the binding energy of interactions, electrostatic-potential surface (ESP) and binding sites. All calculations were performed at a fine quality calculation level. Firstly, using DMOL3 and B3LYP hybrid function the molecular structure of the MOF unit was fully relaxed. During calculations, the Multiplicity factor was kept in Auto mode with double numeric plus polarizing (DNP+) basis set and water as solvent. Successively, structural simulation on the relaxed structure was performed to locate the possible interaction site of the anion within the relaxed MOF unit was located using a simulated annealing technique. The electrostatic potential (ESP) on the van der Waals (VDW) surfaces (isodensity = 0.001 a.u.) of the MOF unit was derived based on its ground state electron density.

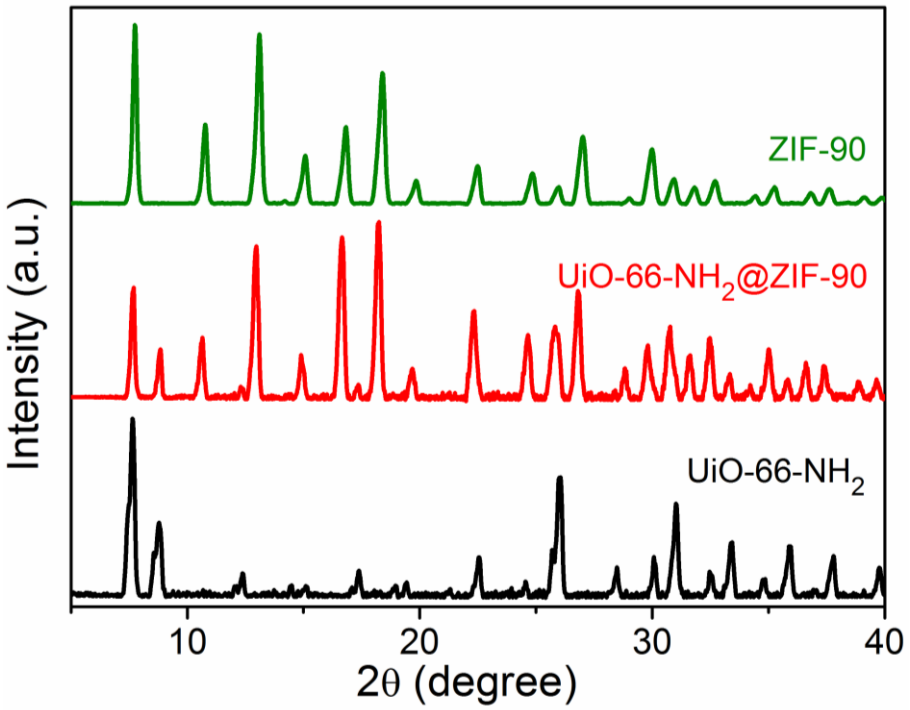

Fig. S1. PXRD patterns of UiO-66-NH_2, UiO-66-NH_2@ZIF-90 and ZIF-90. Characteristics Bragg peaks for both UiO-66-NH_2 and ZIF-90 are present in the composite material.

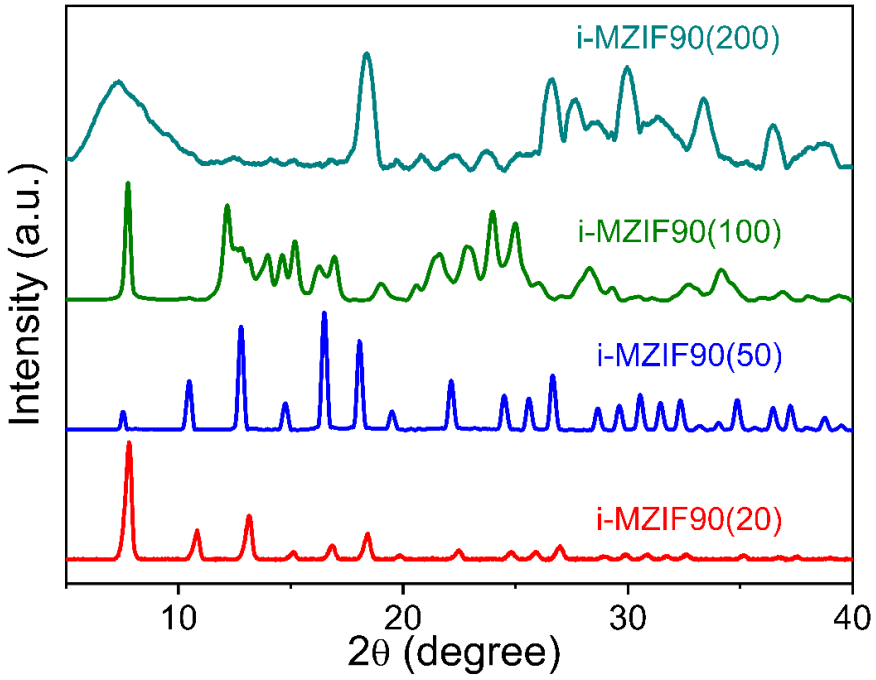

Fig. S2. PXRD patterns of i-MZIF90(20), i-MZIF90(50), i-MZIF90(100) and i-MZIF90 (200).

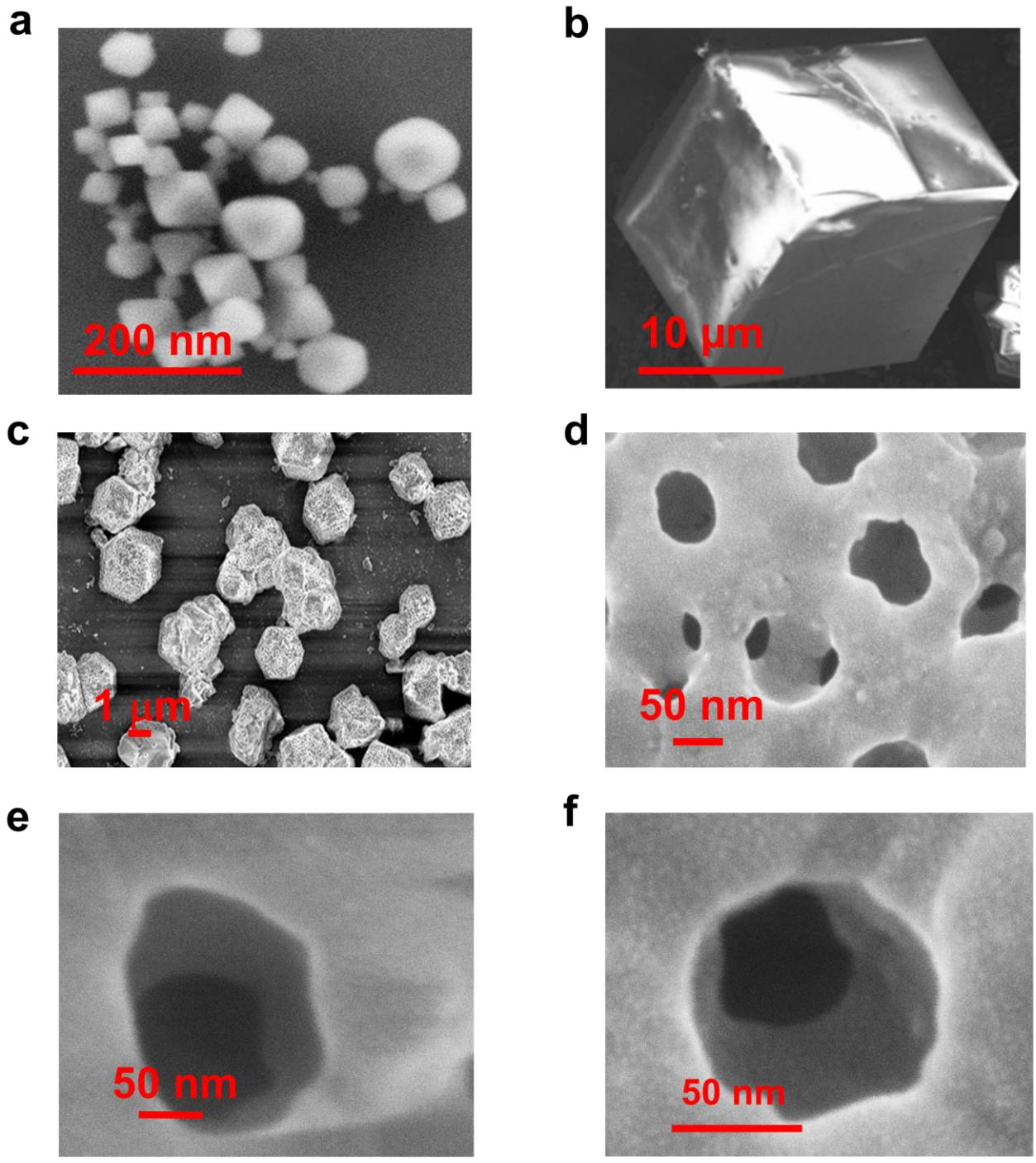

Fig. S3. FESEM image of **a,** UiO-66-NH_2, **b,** ZIF-90 **c-f,** i-MZIF90(50).

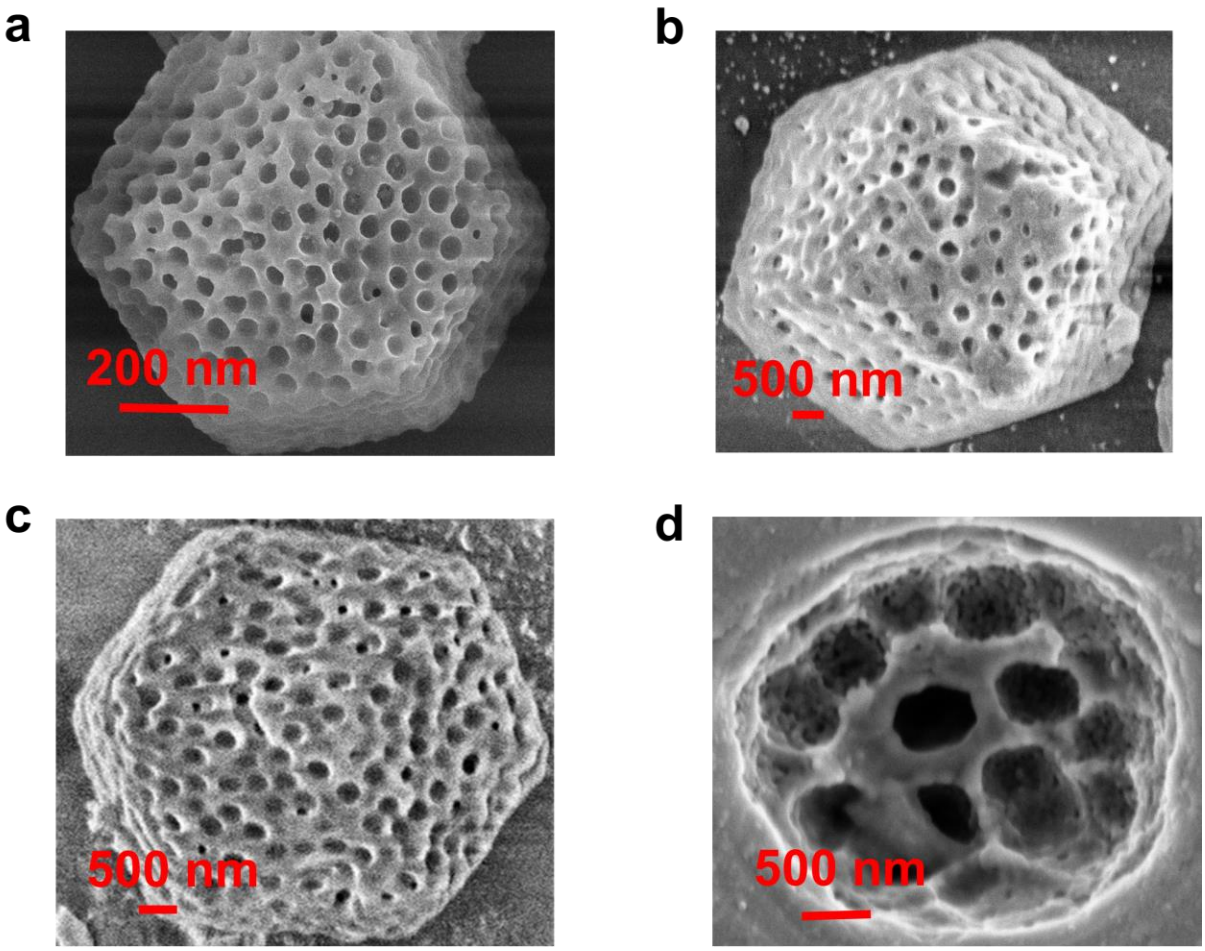

Fig. S4. FESEM images for different pore sized of i-MZIF90(50). **a,** Average size ~86 nm; **b,** Average size ~250 nm, **c,** Average size ~400 nm; **d,** Average size ~650 nm.

Table S1. EDX analysis of ZIF-90.

Element	Weight %	Atomic %
C K	38.63	54.76
N K	20.13	24.47
O K	12.48	13.28
Zn L	28.76	7.49
Totals	**100.00**	**100.00**

Table S2. EDX analysis of UiO-66-NH_2@ZIF-90 composite.

Element	Weight%	Atomic%
C K	39.60	58.94
N K	14.63	18.67
O K	12.64	14.13
Zn L	22.80	6.24
Zr L	10.32	2.02
Totals	**100.00**	**100.00**

Table S3. EDX analysis of UiO-66-NH_2@ZIF-90 composite after 12 hours of base treatment.

Element	Weight%	Atomic%
C K	44.69	58.86
N K	16.84	19.02
O K	17.77	17.99
Zn L	14.02	3.39
Zr L	6.68	0.74
Totals	100.00	100.00

Table S4. EDX analysis of UiO-66-NH_2@ZIF-90 composite after 24 hour of base treatment.

Element	Weight%	Atomic%
C K	46.02	59.97
N K	16.09	17.35
O K	19.94	19.34
Zn L	15.36	3.36
Zr L	2.41	0.48
Totals	100.00	100.00

Table S5. EDX analysis of UiO-66-NH_2@ZIF-90 composite after 72 hours of base treatment.

Element	Weight%	Atomic%
C K	48.46	60.17
N K	15.61	16.62
O K	21.33	19.88
Zn L	14.57	3.32
Zr L	0.03	0.00
Totals	100.00	100.00

Element	Weight %	Atomic %
C K	48.46	60.17
N K	15.61	16.62
O K	21.33	19.88
Zn L	14.57	3.32
Zr L	0.03	0.00
Totals	100.00	100.00

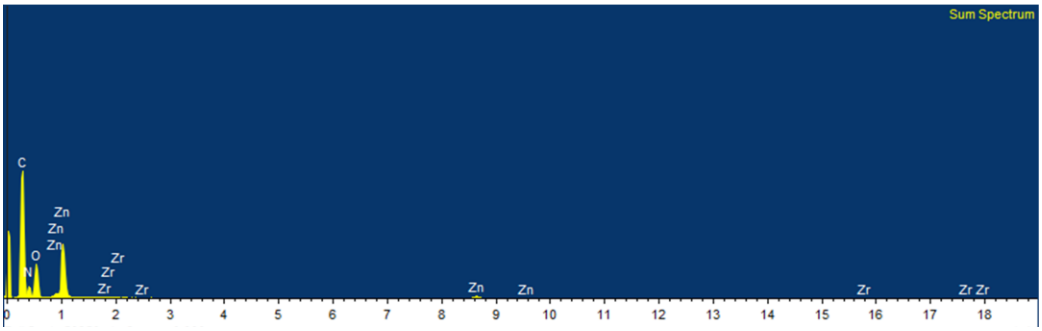

Fig. S5. EDX analysis of i-MZIF90(50).

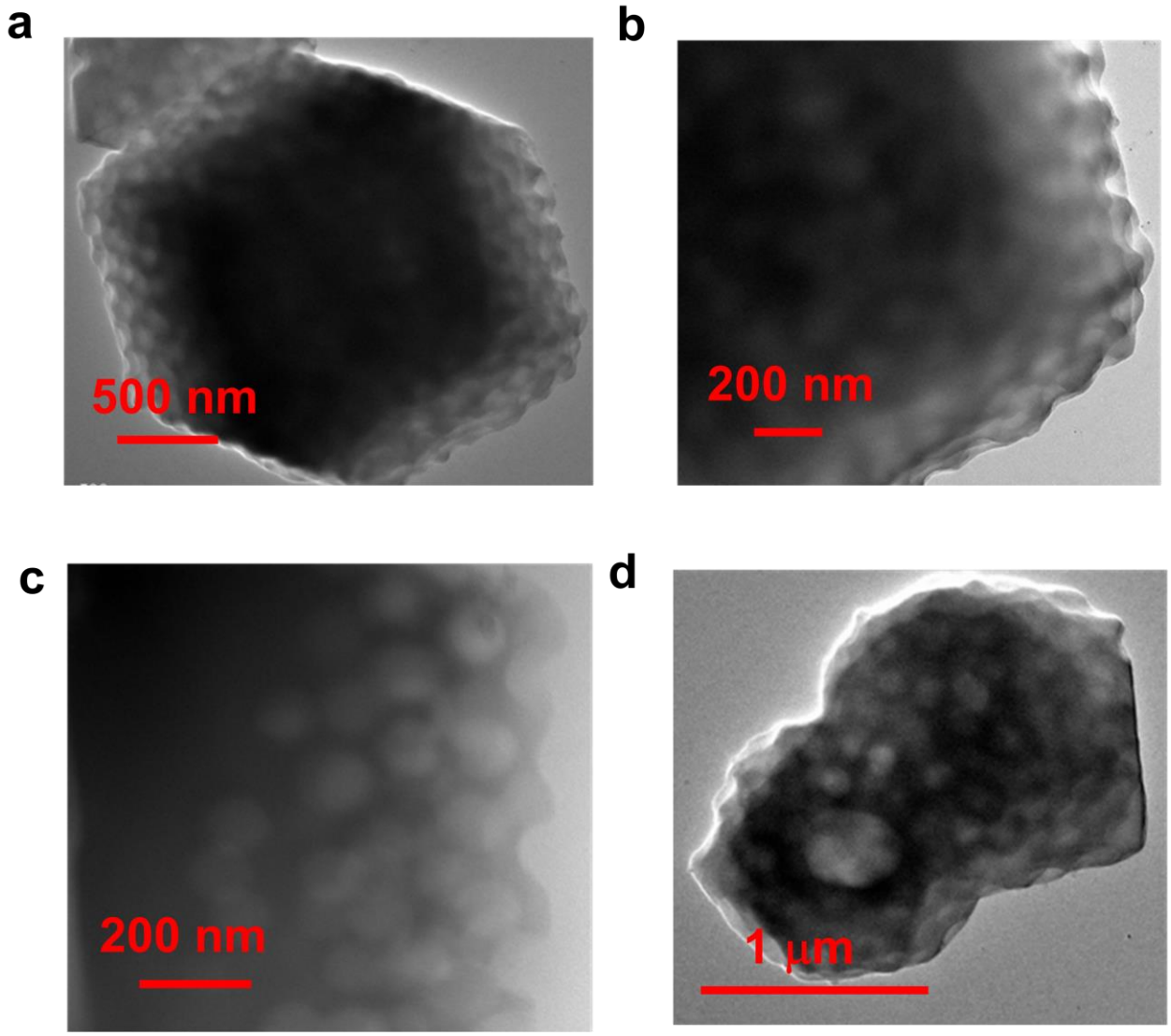

Fig. S6. TEM images of i-MZIF90(50) from **a** to **d**.

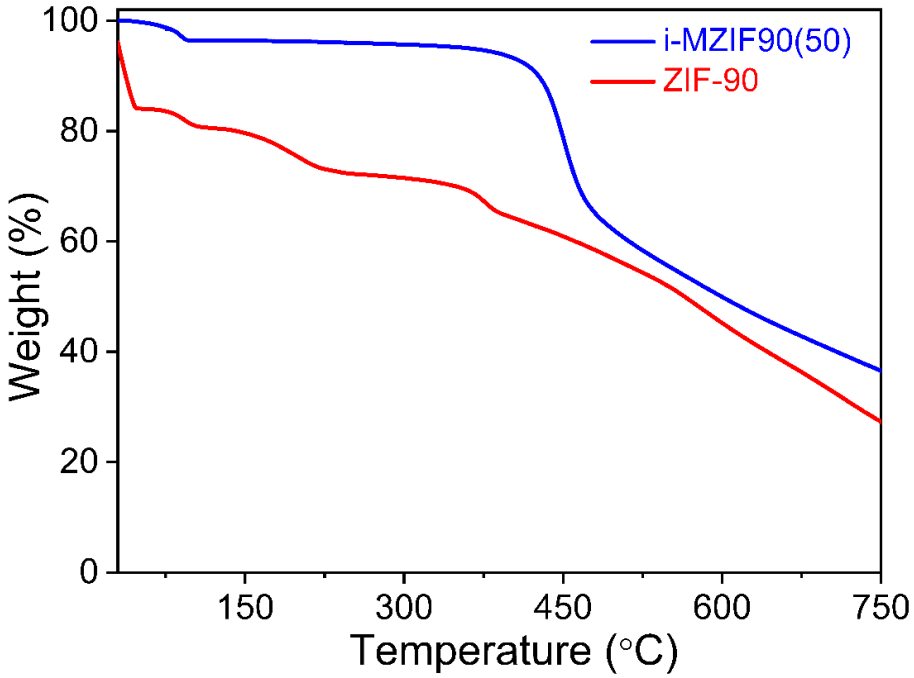

Fig. S7. TGA curves of ZIF-90 and i-MZIF90(50).

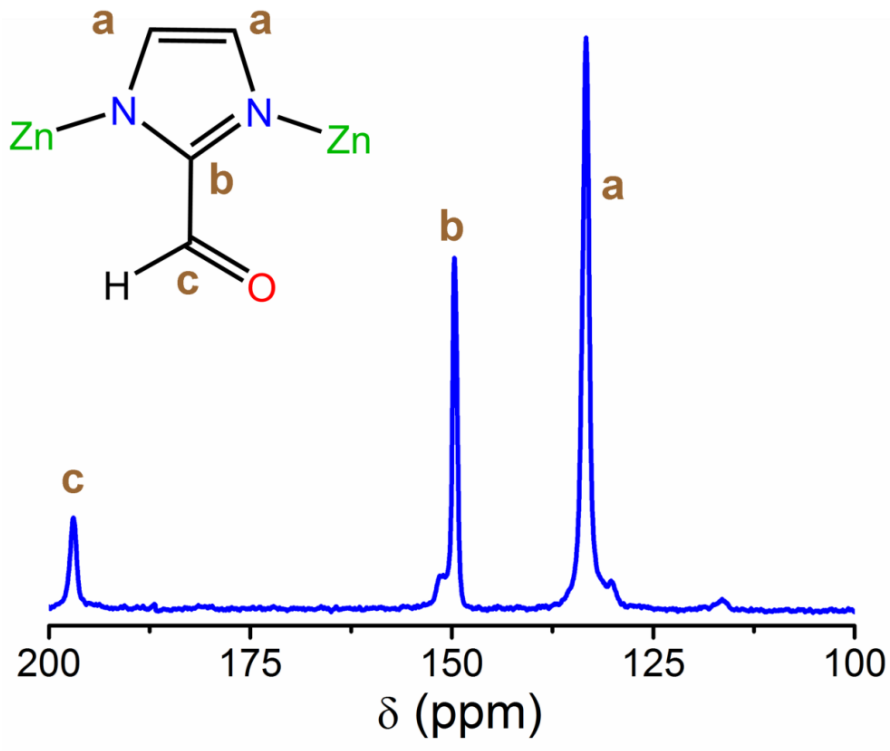

Fig. S8. ^{13}C solid state NMR of ZIF-90.

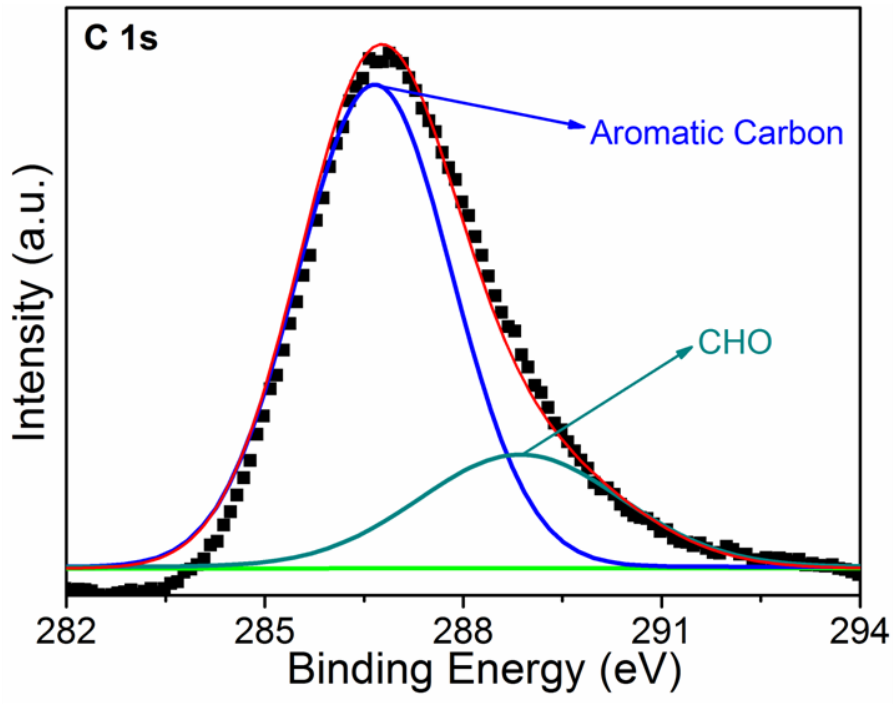

Fig. S9. High resolution XPS spectra of C 1s. ZIF-90.

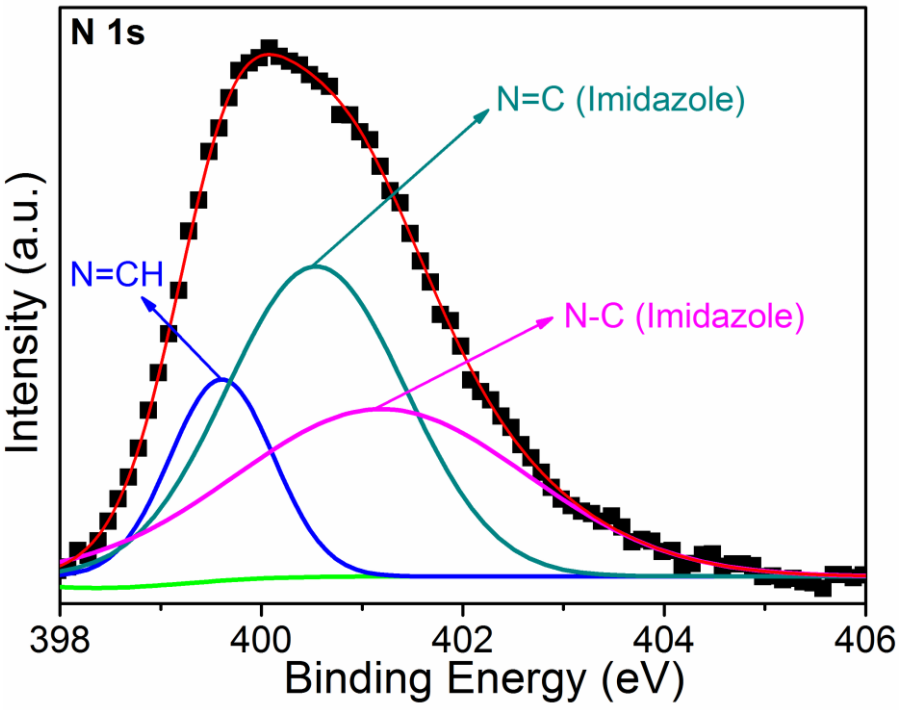

Fig. S10. XPS spectra of N 1s for i-MZIF90(50).

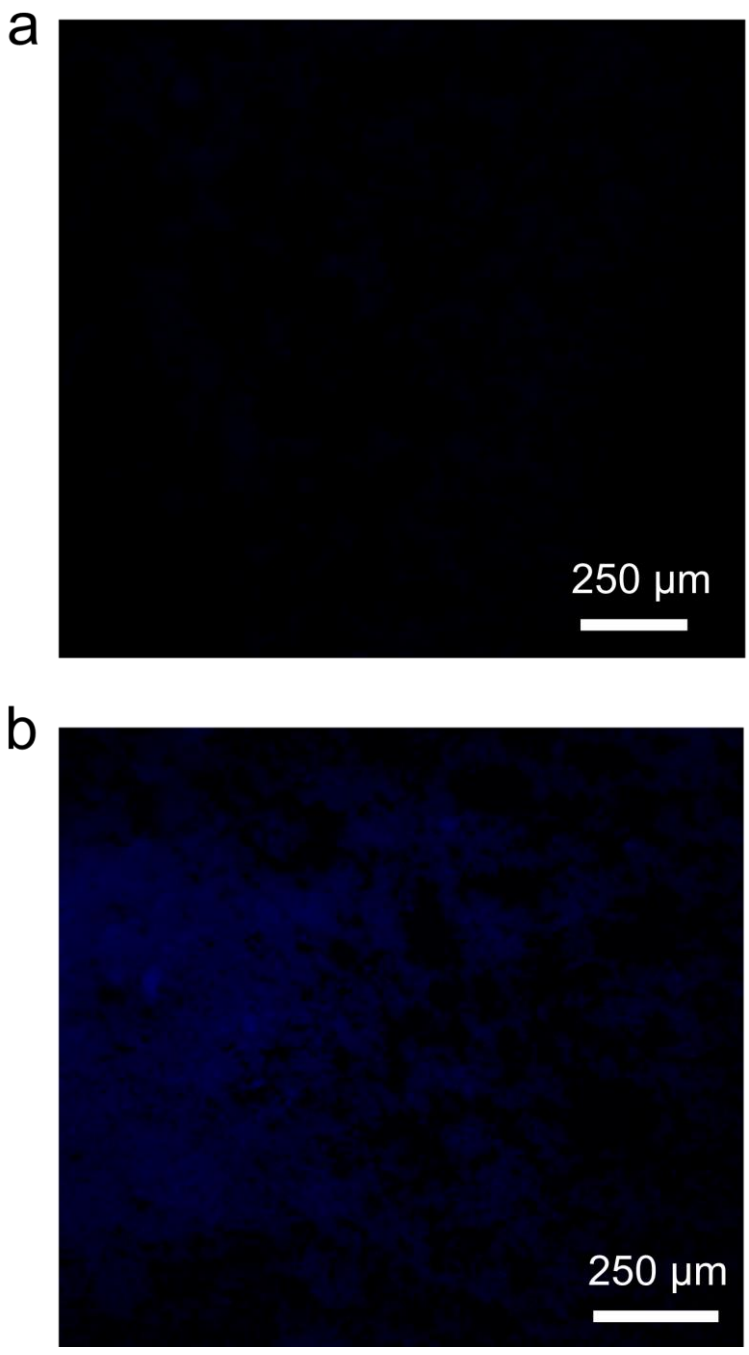

Fig. S11. Fluorescence imaging of **a,** ZIF-90 and **b,** i-MZIF90(50).

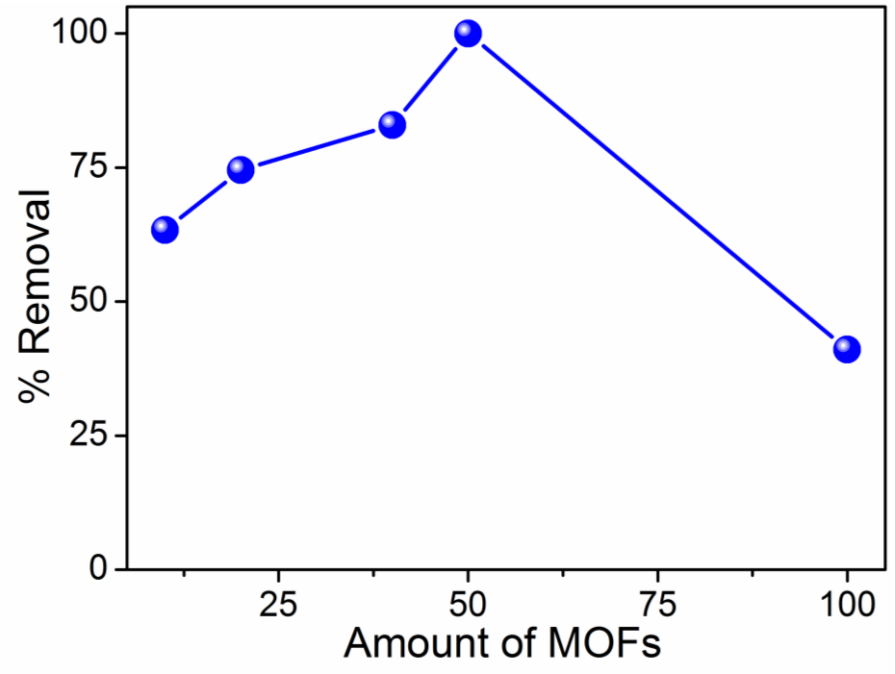

Fig. S12. U capture studies were carried out using different macroporous MOFs: i-MZIF90(10), i-MZIF90(20), i-MZIF90(40), i-MZIF90(50) and i-MZIF90(100). The i-MZIF90(50) shows highest capture efficiency compared to other macroporous materials. The duration of capture study was 2 h.

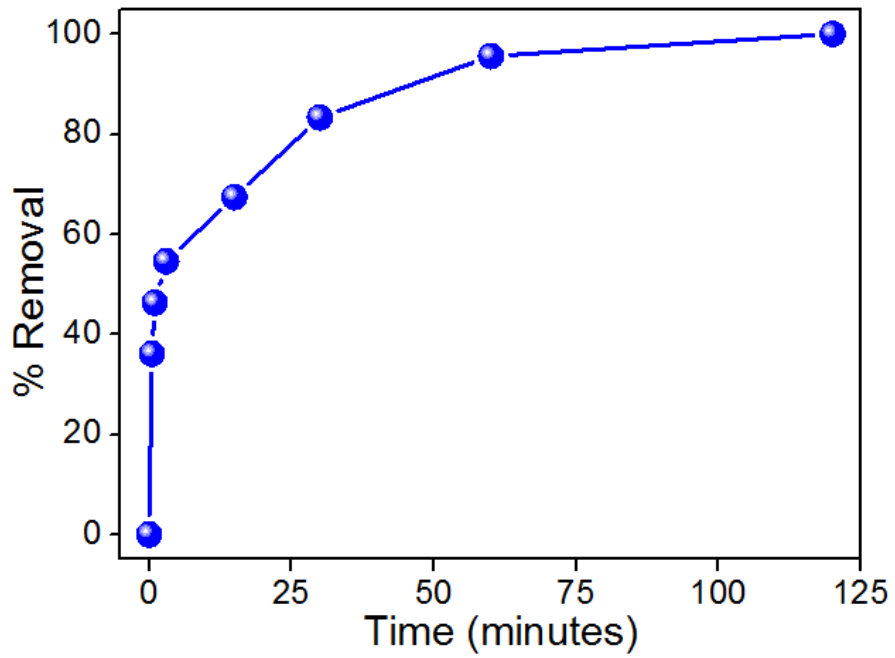

Fig. S13. Removal % of U at different time intervals by i-MZIF90(50) from U spiked deionised water at V/m = 1500 mL g^{-1}.

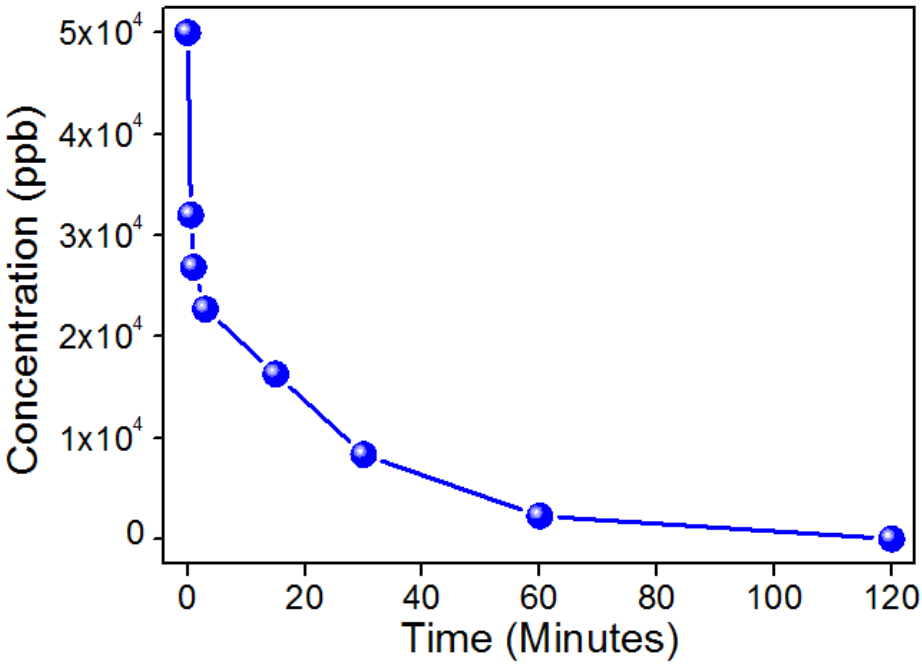

Fig. S14. Kinetics of U removal efficiency by i-MZIF90(50) from water spiked with U (50000 ppb) at V/m = 1500 mL g^{-1}.

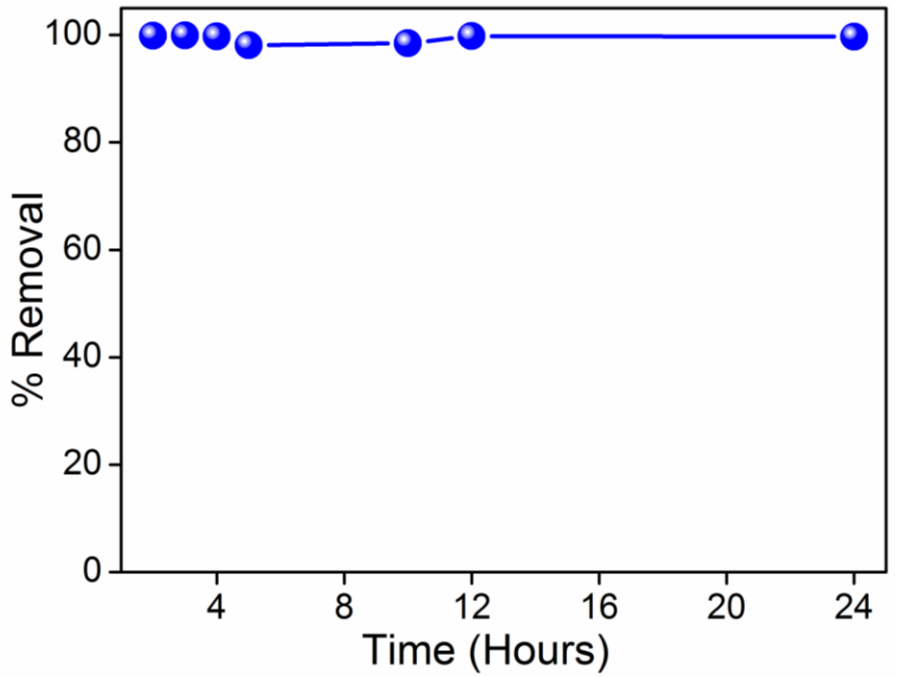

Fig. S15. Leaching test of U from i-MZIF90(50) with time.

Table S6. Comparison of this work with other related investigations of U extraction for various adsorbents from U spiked water.

Adsorbents	Type	Contact Time	Reference
i-MZIF90(50)	MOF	120 min	This work
COF-TpDb-AO	COF	180 min	*Adv. Mater.*, 2018, **30**, 1705479
PPA@MISS-PAF-1	Composite	180 min	*Chem*, 2020, **6**, 1683
MISS-PAF-1	PAF	200 min	*ACS Cent. Sci.*, 2019, **5**, 1432
USC-CP-1	MOF	800 min	*Angew. Chem. Int. Ed.*, 2019, **58**, 18808
FJSM-SnS	Layered Hybrid Thiostannate	1200 min	*J. Am. Chem. Soc.*, 2016, **138**, 12578
PIDO NF	Fiber	1400 min	*Adv. Energy Mater.*, 2018, **8**, 1802607
SMON-PAO	Fiber	1600 min	*Adv. Funct. Mater.*, 2019, **29**, 1805380
BP-PAO	Black Phosphorous	48 h	*Angew. Chem. Int. Ed.*, 2020, **59**, 1220
Zn^{2+}-PAO hydrogel	Hydrogel	100 h	*Adv. Mater.*, 2020, **32**, 1906615

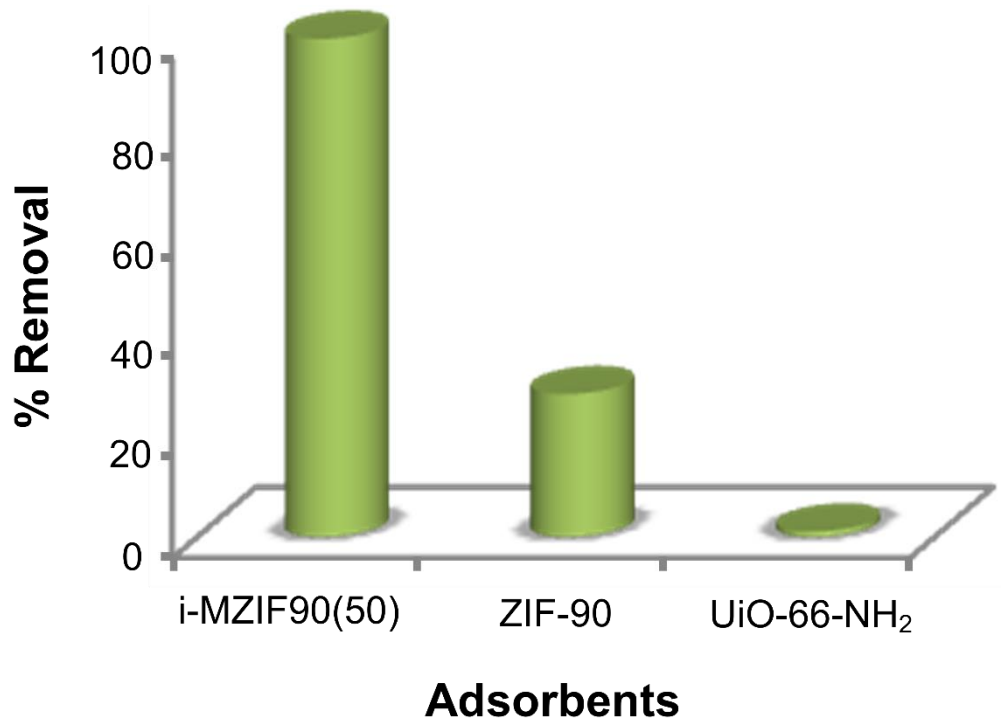

Fig. S16. Removal % of U by i-MZIF90(50), ZIF-90 and UiO-66-NH_2. The duration of capture study was 2 h.

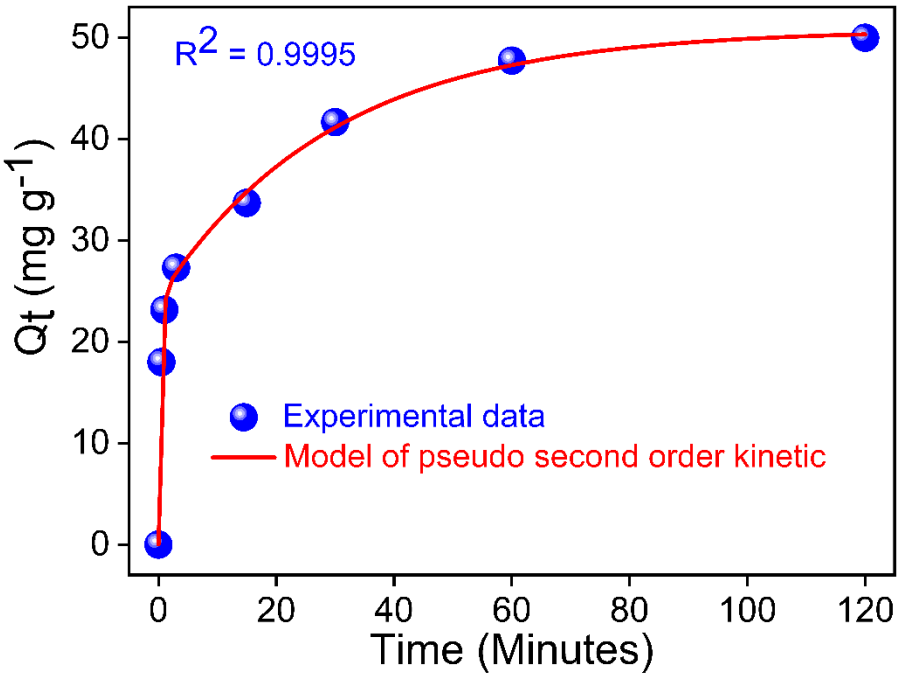

Fig. S17. The uranium sorption follows the pseudo-second-order kinetics, implying that the adsorption of uranyl ions onto i-MZIF90(50) was chemical interactions.

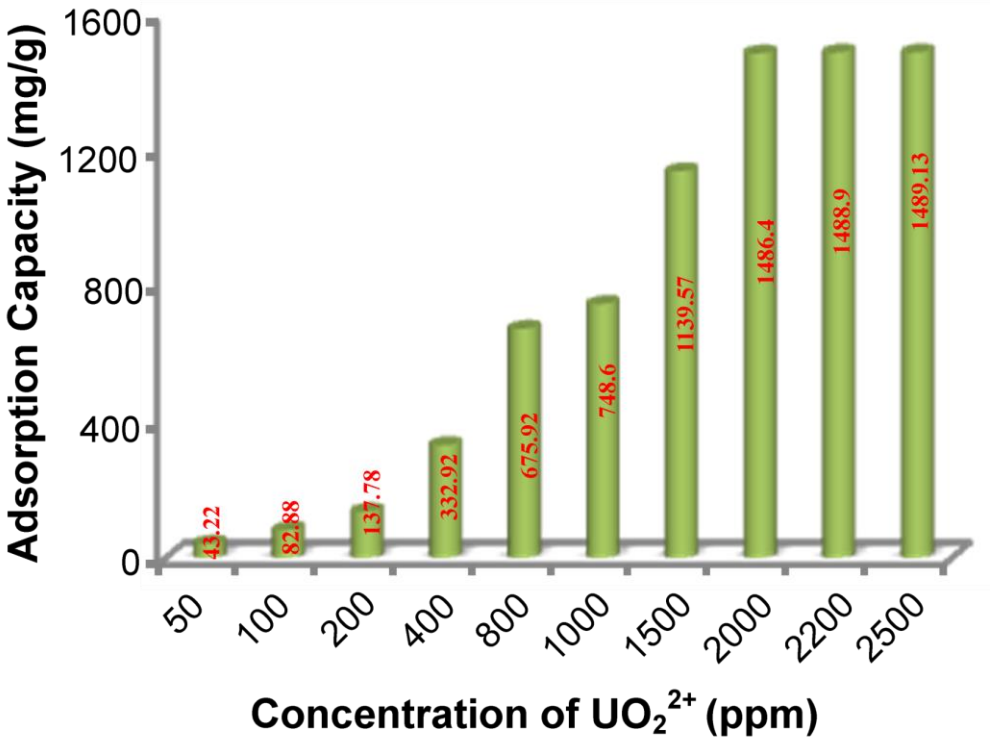

Fig. S18. Concentration-dependent adsorption capacities for i-MZIF90(50).

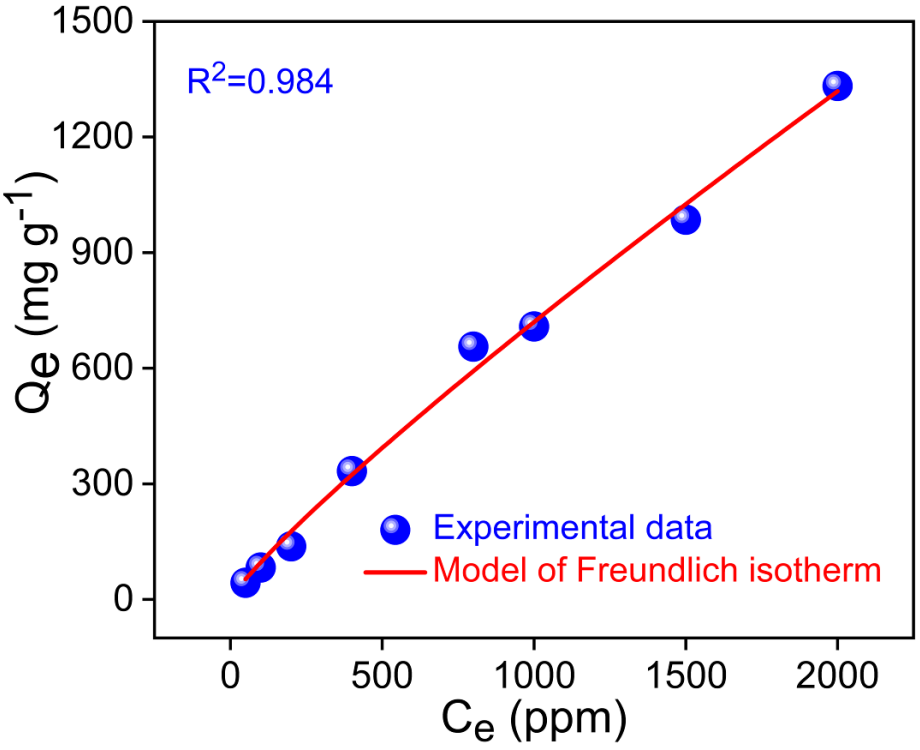

Fig. S19. Freundlich adsorption isotherm for i-MZIF90(50).

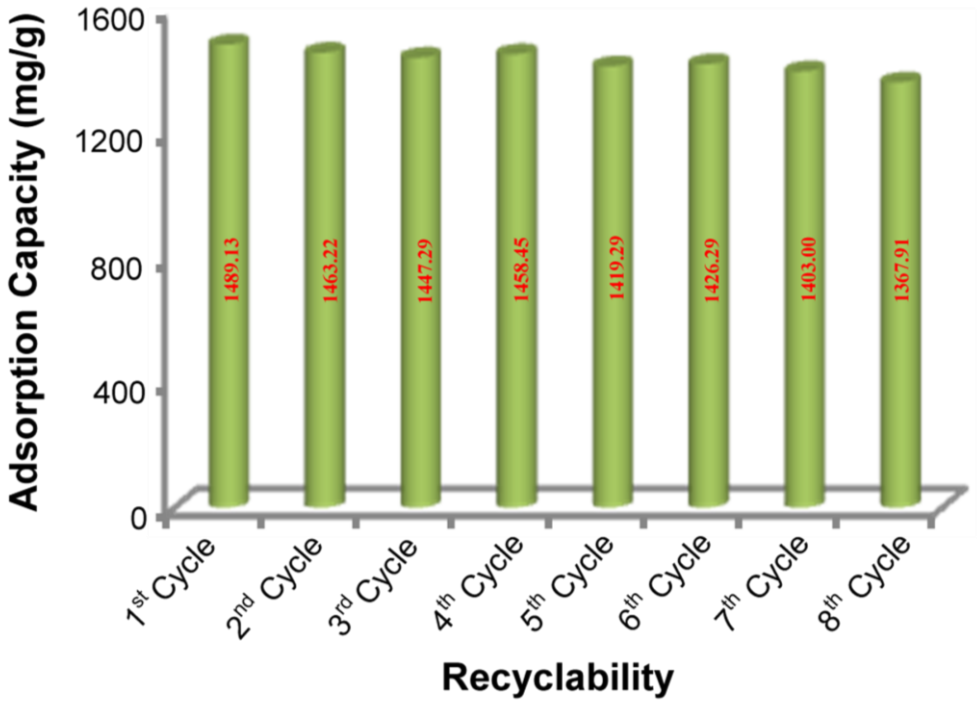

Fig. S20. U recyclability test for i-MZIF90(50) from deionized water.

Table S7. Adsorption capacity and elution efficiency (%) of i-MZIF90(50) in each cycle during the U recyclability test from deionized water.

Cycle Number	Adsorption Capacity (mg/g)	Elution Efficiency (%)
1	1489.13	100
2	1463.22	98.26
3	1447.29	97.19
4	1458.45	97.94

5	1419.29	95.31
6	1426.29	95.78
7	1403	94.22
8	1367.91	91.86

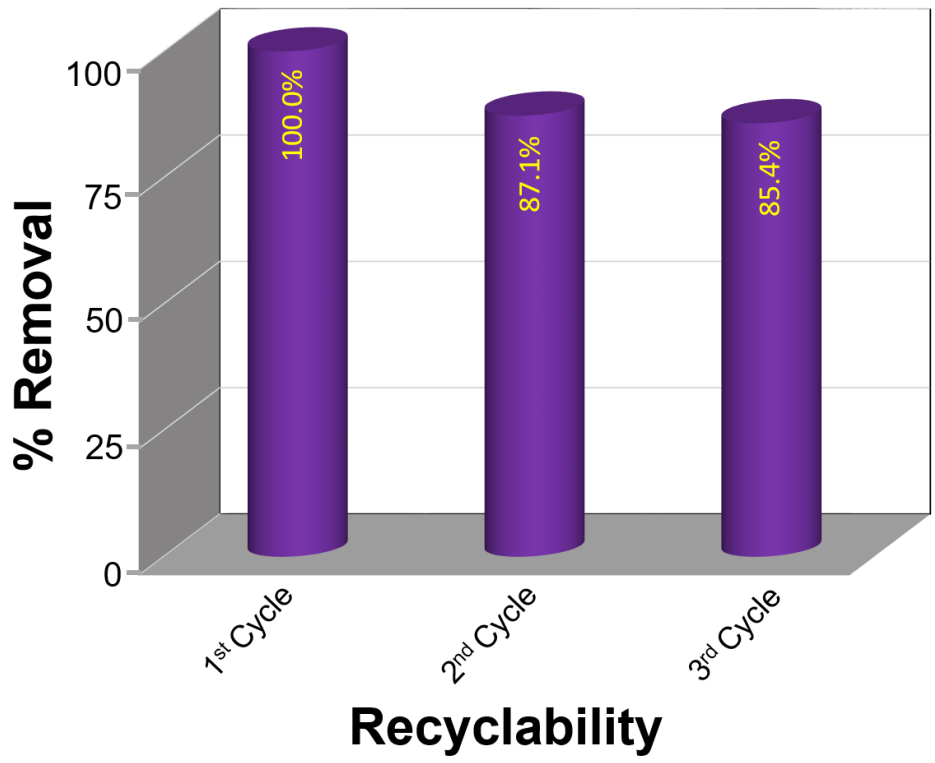

Fig. S21. Recyclability test of i-MZIF90(50) for U recovery from spiked natural seawater at V/m 2000 mg g^{-1}.

Table S8. Adsorption capacity and elution efficiency (%) of i-MZIF90(50) in each cycle during the recyclability test in spiked seawater.

Cycle Number	Adsorption Capacity (mg/g)	Elution Efficiency (%)
1	193.7	100
2	168.7	87.1
3	165.4	85.4

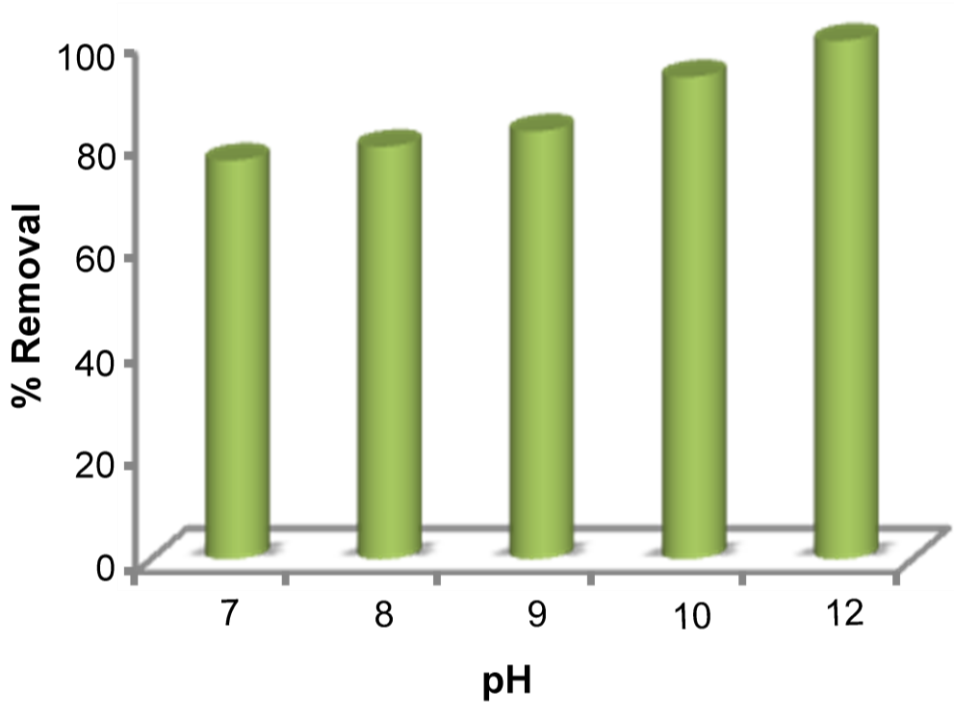

Fig. S22. Bar diagram representing relative % removal of U from aqueous solution by i-MZIF90(50) at different pH at V/m = 2000 mL g^{-1}.

Table S9. Comparison of this work with other related investigations of U extraction for various adsorbents from U spiked water.

Adsorbents	Type	Capacity (mg/g)	Distribution Coefficient (K_d)	Reference
i-MZIF90(50)	MOF	1489.13	1.24 x 10^7	This work
Zn^{2+}-PAO hydrogel	Hydrogel	1188	-	*Adv. Mater.*, 2020, **32**, 1906615
PIDO NF	Fiber	1187.05 ± 28.45	2.84 x 10^5	*Adv. Energy Mater.*, 2018, **8**, 1802607
SMON-PAO	Fiber	1089.36 ± 64.31	3.75 x 10^6	*Adv. Funct. Mater.*, 2019, **29**, 1805380
HTC-AO	Carbon	1021.6	0.5 x 10^4	*J. Mater. Chem. A*, 2014, **2**, 1550
BP-PAO	Black Phosphorous	990.60 ± 37.39	-	*Angew. Chem. Int. Ed.*, 2020, **59**, 1220
UCY-13	MOF	984	-	*J. Mater. Chem. A*, 2020, **8**, 1849
PIDO/Alg	Hydrogel	910.98	1.72 x 10^4	*Adv. Funct. Mater.*, 2019, **29**, 1901009
COF-SO_3H	COF	851 mg	9.8 x 10^6	*Adv. Sci.*, 2019, **6**, 1900547
USC-CP-1	MOF	562	-	*Angew. Chem. Int. Ed.*, 2019, **58**, 18808
POP-*o*NH_2 -AO	POP	530	8.18 x 10^5	*Nat. Commun.*, 2018, ***9***, 1644
TFPT-BTAN-AO	COF	427	8.36 x 10^6	*Nat. Commun.*, 2020, **11**, 436
COF-TpDb-AO	COF	398.4	2.2 x 10^8	*Adv. Mater.*, 2018, ***30***, 1705479
KMS-1	Layered Metal Sulfide	382	1.5-4.8 x 10^4	*J. Am. Chem. Soc.*, 2012, **134**, 16441

FJSM-SnS	Layered Hybrid Thiostannate	338.43	2.64 x 10^4	*J. Am. Chem. Soc.*, 2016, **138**, 12578
MIL-101(Cr)-traiziole-COOH	MOF	314	1.8 x 10^4	*ACS Appl. Mater. Interfaces*, 2016, **8**, 31032
PPA@MISS-PAF-1	Composite	307.3	2.18 x 10^7	*Chem*, 2020, **6**, 1683
H-ABP	Fiber	302	-	*Energy Environ. Sci.*, 2019, **12**, 1979
MISS-PAF-1	PAF	253	1.4 x 10^7	*ACS Cent. Sci.*, 2019, ***5***, 1432
H_2BHT	Supramolecular Chelator	105	-	*Nat. Commun.*, 2019, **10**, 819

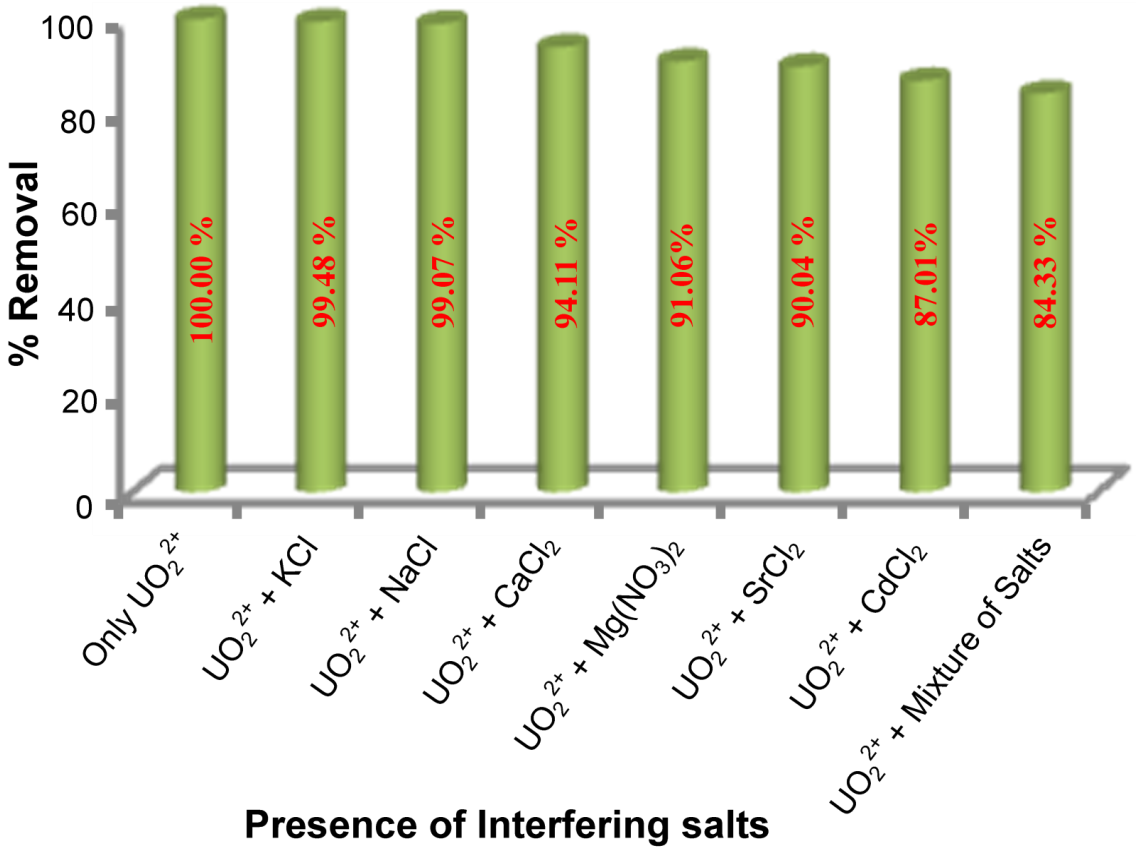

Fig. S23. Removal % of U from a binary as well as mixture of equal concentration of various interfering cations by i-MZIF90(50) at V/m = 1000 mL g^{-1}.

Table S10. The distribution coefficient (K_d) value calculated from a 5 ppm U spiked solution for i-MZIF90(50) at V/m = 1000 mL g^{-1}.

Analytes	**Distribution Constant (K_d)**	**Selectivity (K_d^U/K_d^M)**
Only UO_2^{2+}	1249 x 10^4	-
KCl	19.1 x 10^4	65.4
NaCl	10.7 x 10^4	116.7
$CaCl_2$	1.60 x10^4	780.6
$Mg(NO_3)_2$	1.02 x 10^4	1224.5
$SrCl_2$	0.90 x10^4	1387.8
$CdCl_2$	0.67 x 10^4	1864.2
Mixture of Salts	0.58 x 10^4	2153.4

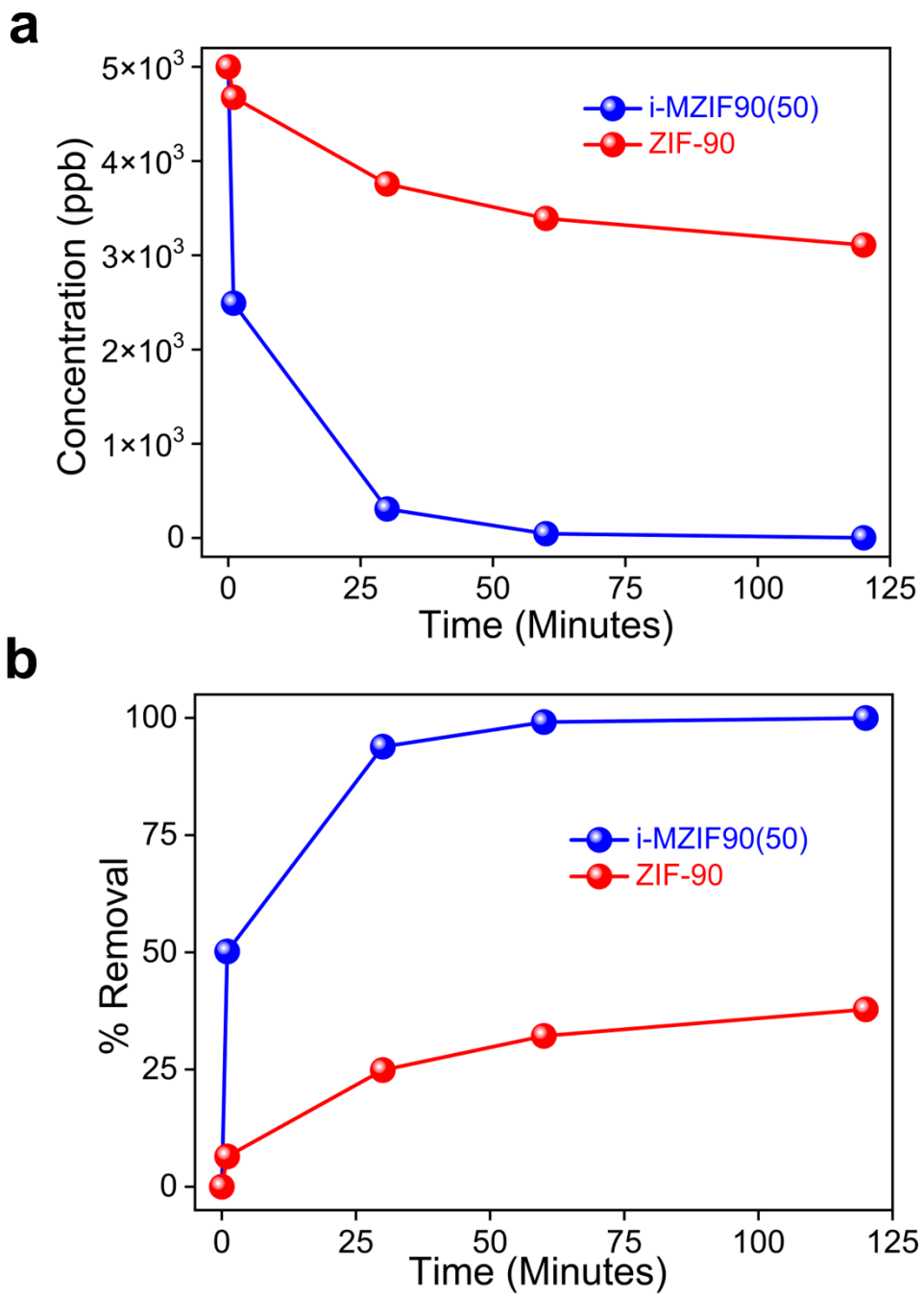

Fig. S24. Recovery of U from 5 ppm U spike potable water at a V/m = 3500 mL g^{-1} by ZIF-90 and i-MZIF90(50). **a,** Decrease in the concentration of U from water. **b,** Removal % in different time interval.

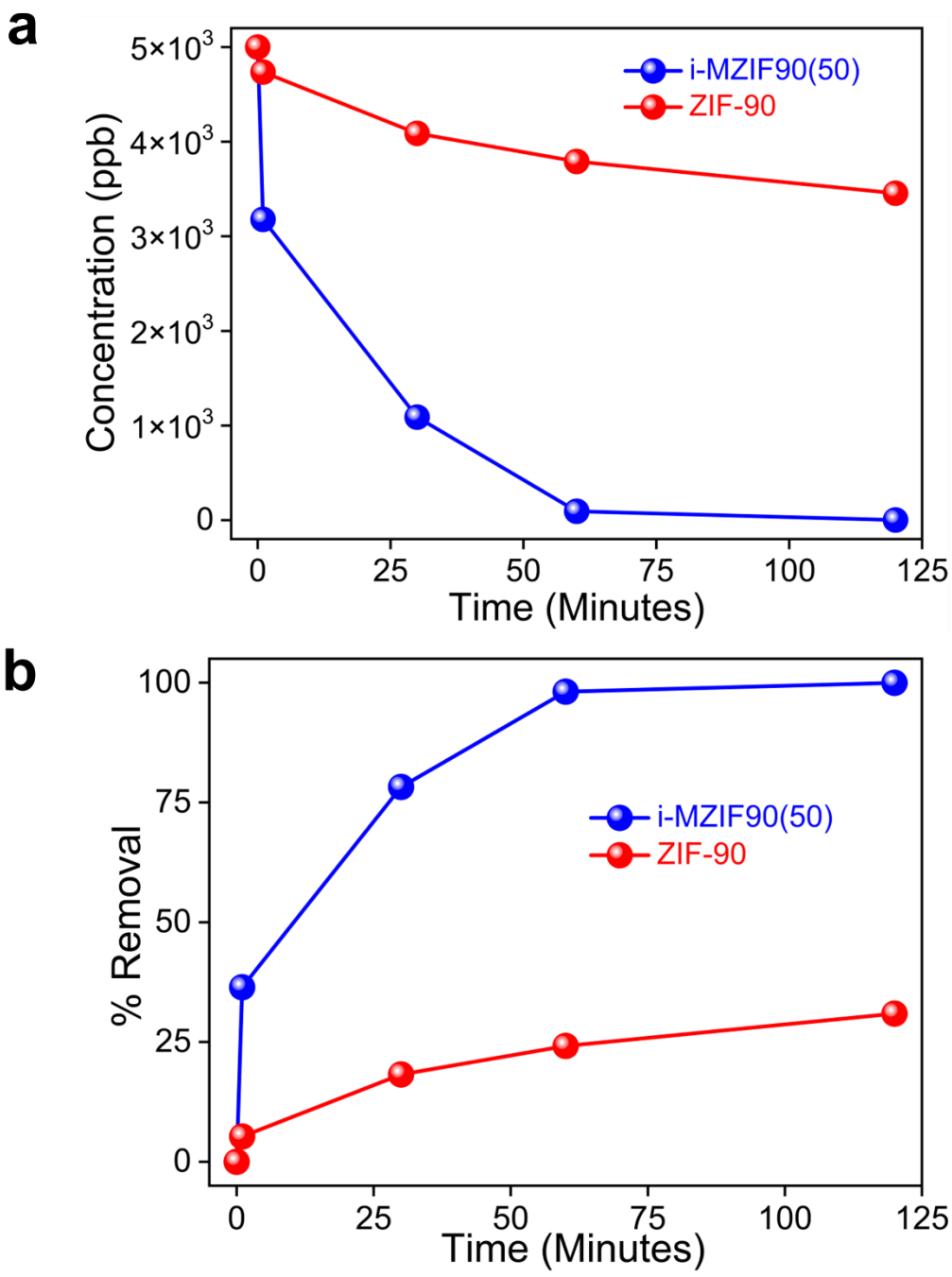

Fig. S25. Recovery of U from 5 ppm U spike lake water at a V/m = 3500 mL g^{-1} by ZIF-90 and i-MZIF90(50). **a,** Decrease in the concentration of U from water. **b,** Removal % in different time interval.

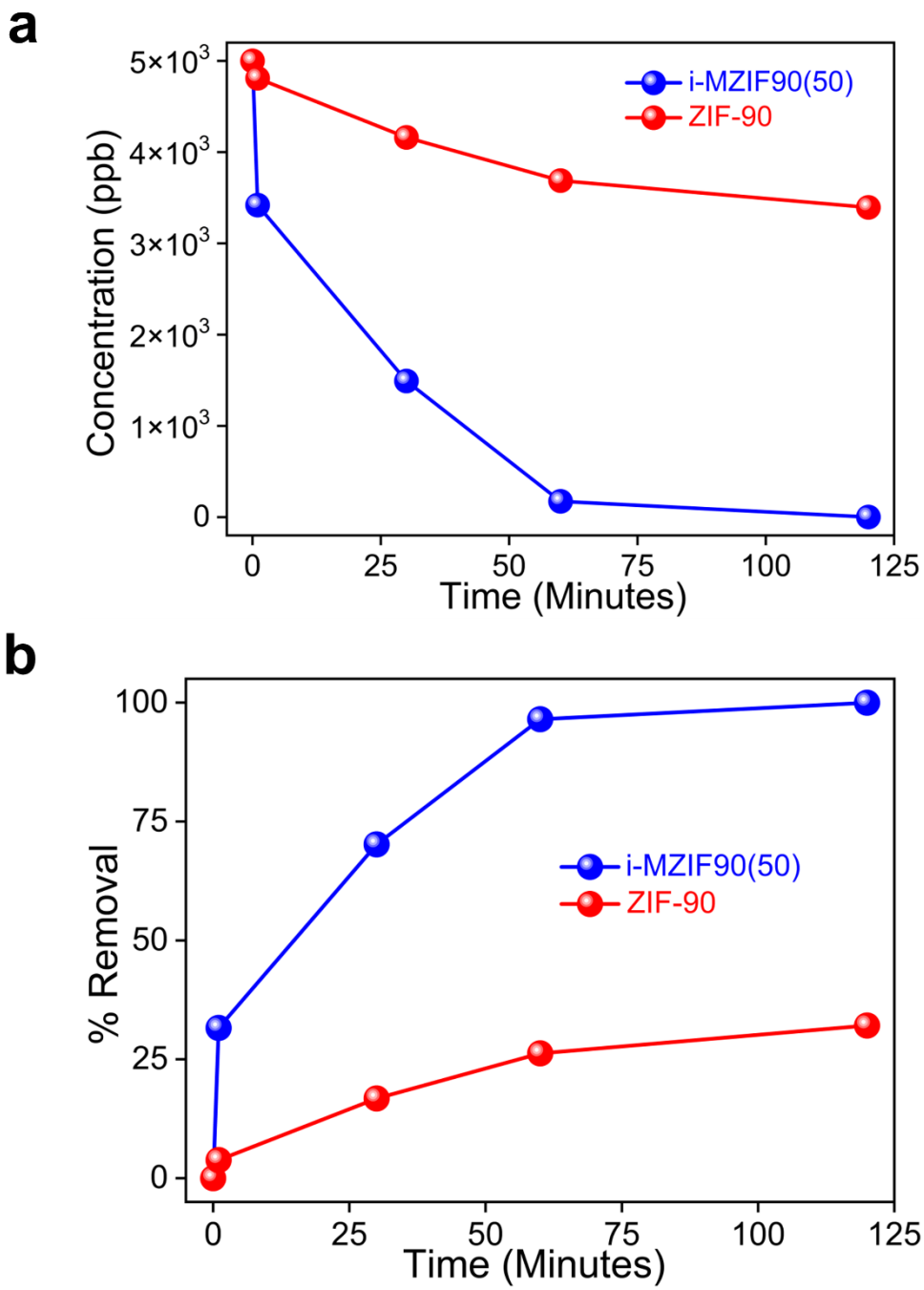

Fig. S26. Recovery of U from 5 ppm U spike river water at a V/m = 3500 mL g^{-1} by ZIF-90 and i-MZIF90(50). **a,** Decrease in the concentration of U from water. **b,** Removal % in different time interval.

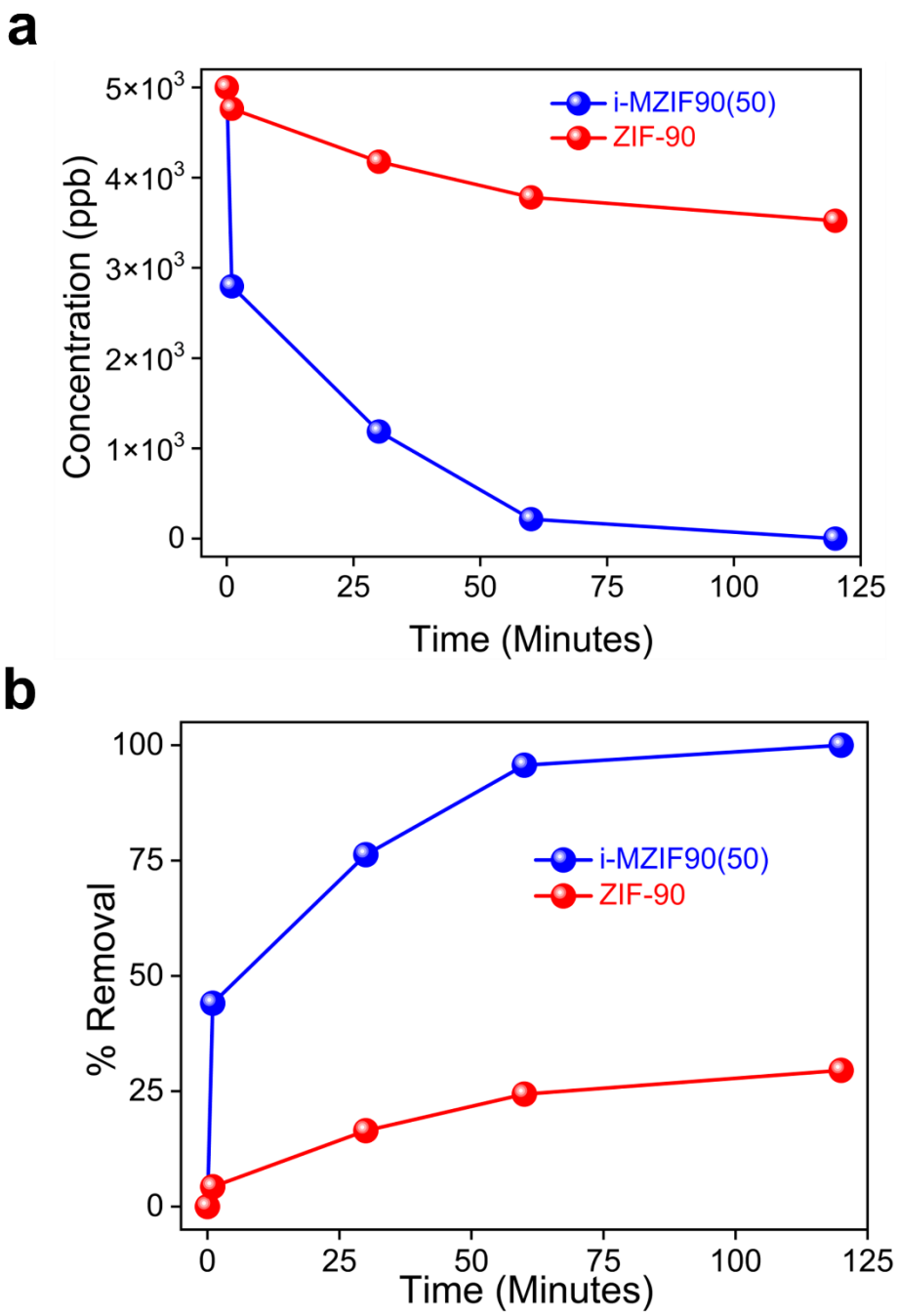

Fig. S27. Recovery of U from 5 ppm U spike artificial seawater at a V/m = 3500 mL g^{-1} by ZIF-90 and i-MZIF90(50). **a,** Decrease in the concentration of U from water. **b,** Removal % in different time interval.

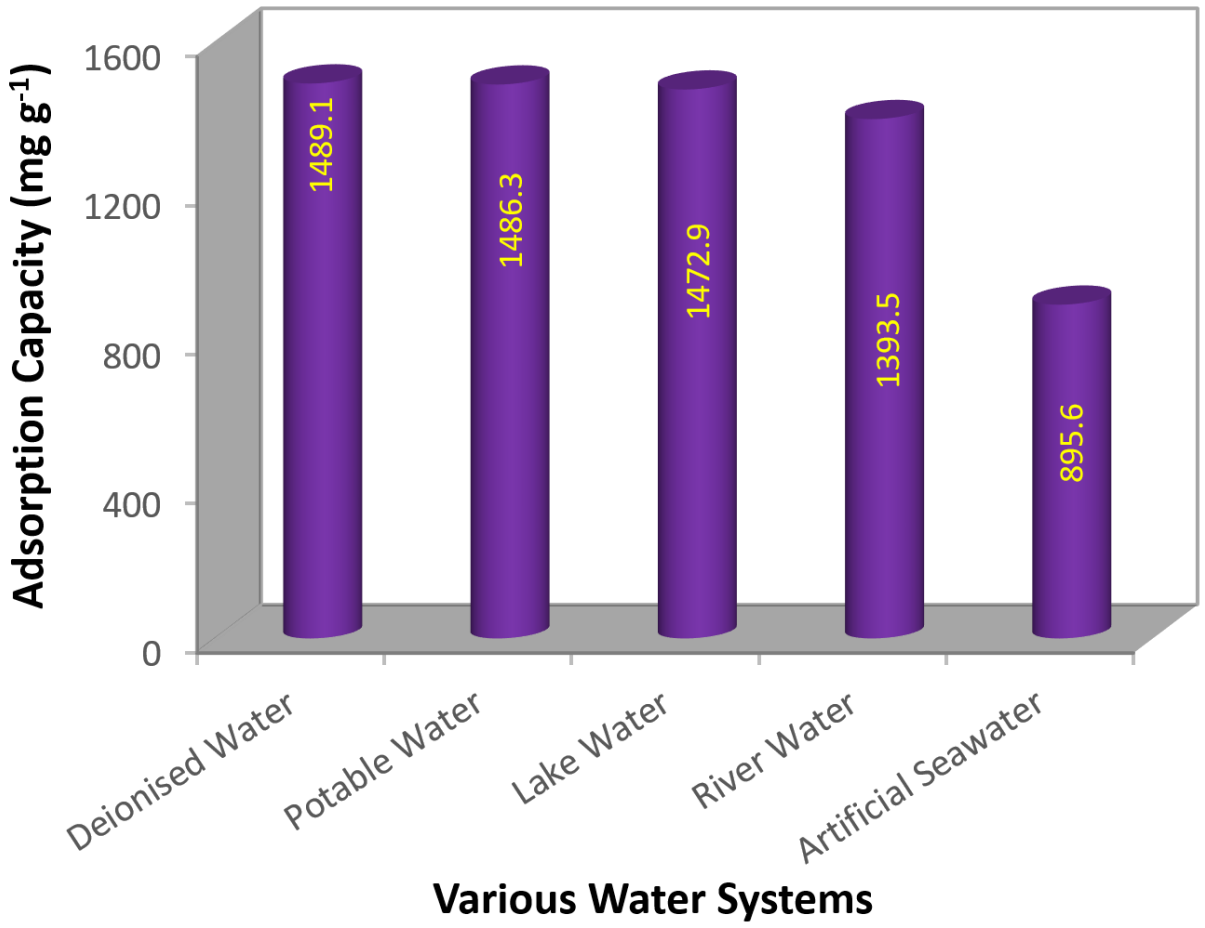

Fig. S28. U Adsorption capacity of i-MZIF90(50) from various U spiked water systems at V/m = 2000 mL g^{-1}.

Table S11. Comparison of this work with other related investigations for U adsorption capacity by i-MZIF90(50) from artificial seawater.

Adsorbents	**Artificial Seawater (mg/g)**	**Reference**
i-MZIF90(50)	895.56	This work
V_2CT	377	*ACS Appl. Mater. Interfaces*, 2016, **8**, 16396
POP-*o*NH_2-AO	290	*Nat. Commun.*, 2018, **9**, 1644

AF series adsorbents	200	*Ind. Eng. Chem. Res.* **2016**, *55*, 4110
ND-AO	121	*ACS Appl. Mater. Interfaces*, 2016, **8**, 28853
Mesoporous Carbon Materials	67	*Ind. Eng. Chem. Res.*, 2013, **52**, 15187

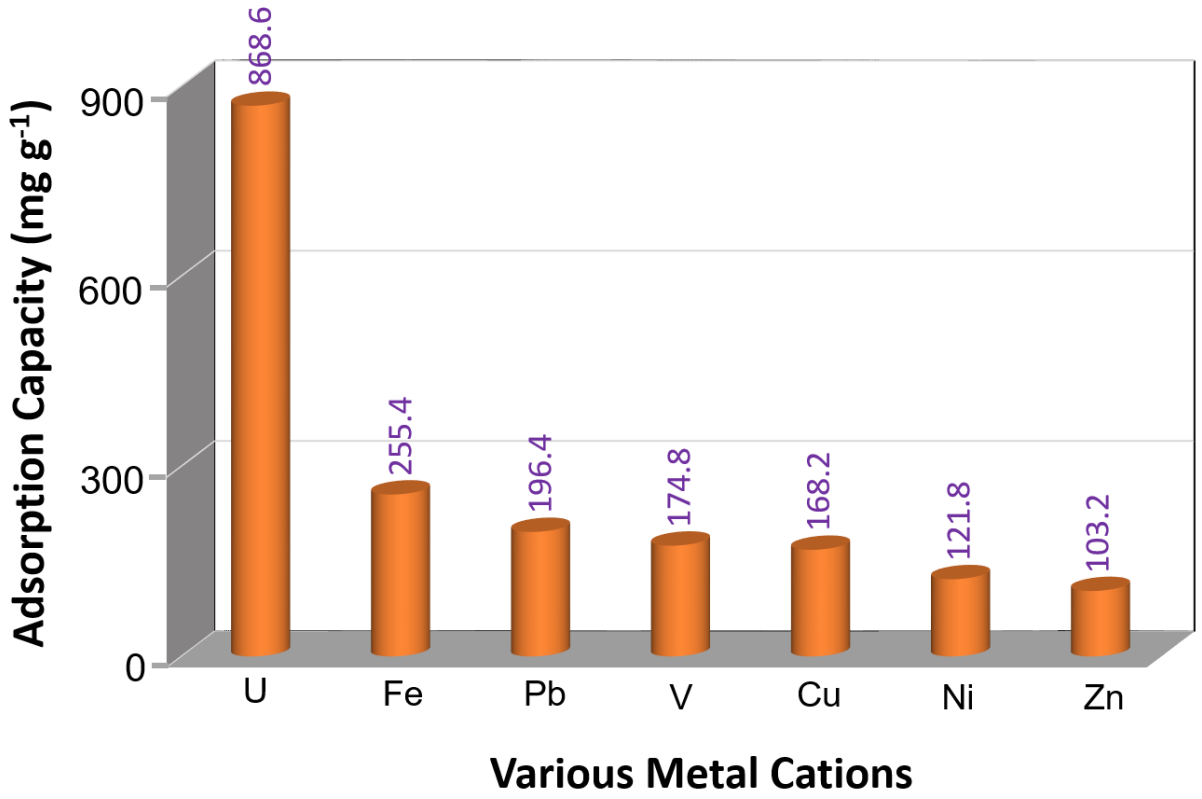

Fig. S29. Adsorption capacity towards different metal cations including U from spiked seawater by i-MZIF90(50) at V/m = 20000 mL g^{-1}.

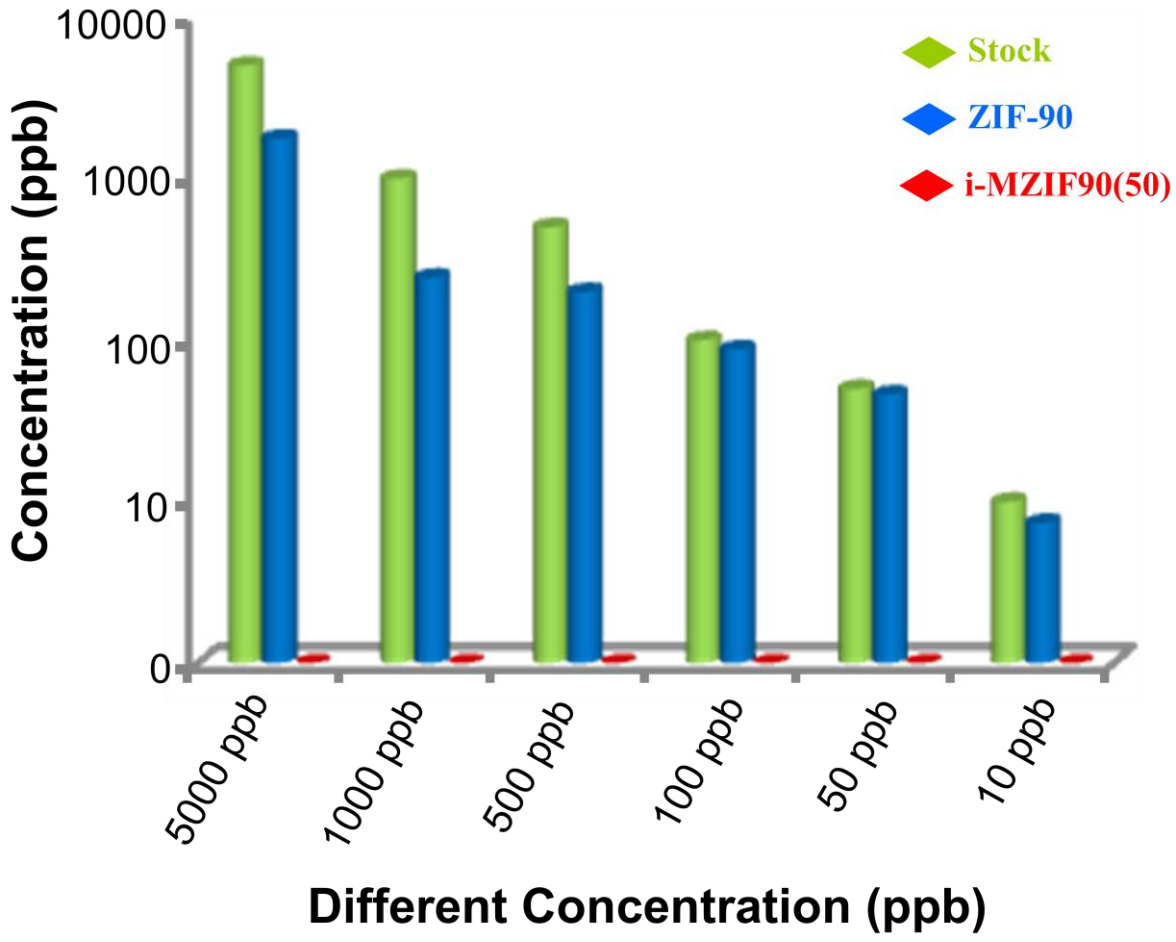

Fig. S30. Comparison between ZIF-90 and i-MZIF90(50) for U recovery from a variety of trace amount of U spiked artificial water at a V/m = 1000 mL g^{-1}.

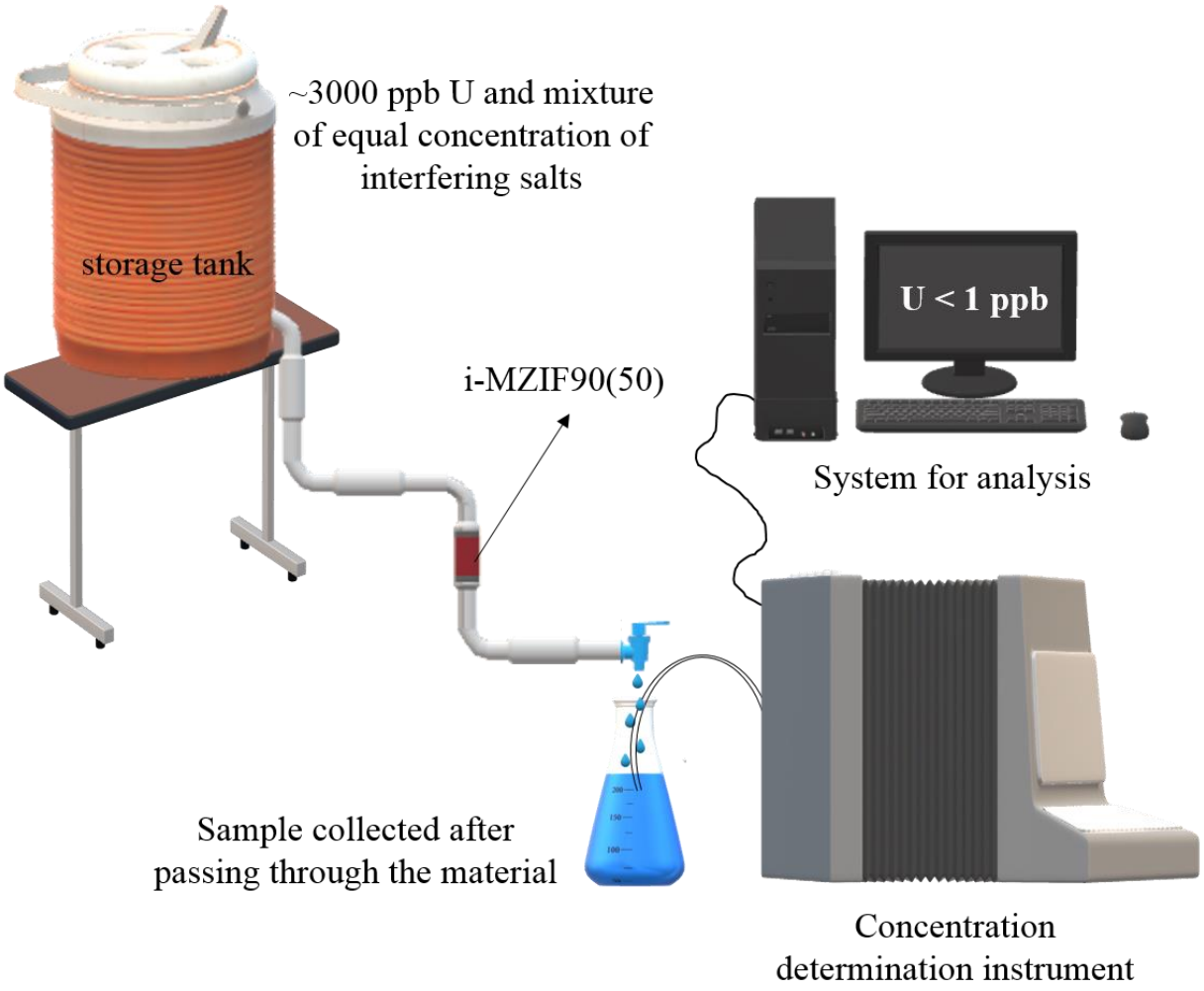

Fig. S31. Schematic representation of the breakthrough experiments of a mixed solution composed of 3-ppm uranium and 3ppm other competitive metal cations containing water by i-MZIF90(50) packed bed.

Table S12. U extraction from natural nonspiked seawater by i-MZIF90(50).

No. of Experiments	U capacity (mg/g)	Average U capacity (mg/g)
Batch 1	26.7	28.2
Batch 2	29.8	
Batch 3	28.3	

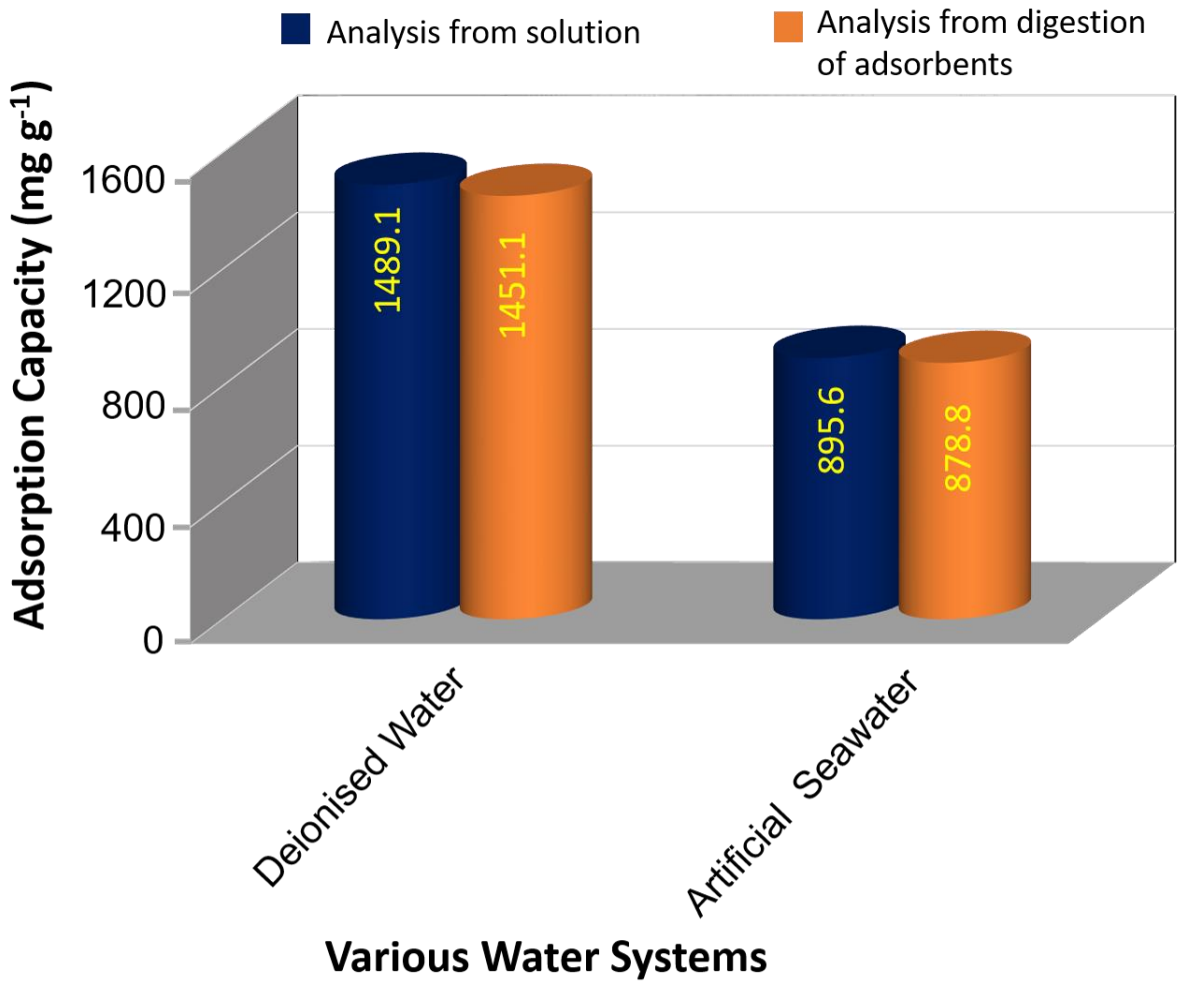

Fig. S32. U adsorption capacity calculation for DI water and artificial seawater from both solution and after digestion of the i-MZIF90(50).

Table S13. Comparison of this work with other related investigations of U extraction from natural nonspiked seawater for various adsorbents.

Serial No.	Adsorbents	Type	Capacity (mg/g)	Time (days)	Reference
1	i-MZIF90(50)	MOF	28.2	25	This work
(*)	COF-SO_3H	COF	17.8	7	*Adv. Sci.*, 2019, **6**, 1900547
2	PPA@MISS-PAF-1	Composite	16.97	90	*Chem*, 2020, **6**, 1683
3	BP-PAO	Black Phosphorus	11.76	56	*Angew. Chem. Int. Ed.*, 2020, **59**, 1220
4	H-ABP	Fiber	11.5	90	*Energy Environ. Sci.*, 2019, **12**, 1979
5	SMON-PAO	Nano Fiber	9.59±0.64	56	*Adv. Funct. Mater.*, 2019, **29**, 1805380
6	Zn^{2+}-PAO	Hydrogel	9.23	28	*Adv. Mater.*, 2020, **32**, 1906615
7	PIDO NF	Fiber	8.7	56	*Adv. Energy Mater.*, 2018, **8**, 1802607
8	MS@PIDO/Alg	Hybrid Sponge	5.84	56	*Adv. Funct. Mater.*, 2019, **29**, 1901009
9	MISS-PAF-1	PAF	5.79	56	*ACS Cent. Sci.*, 2019, ***5***, 1432
10	PPN-6-PAN	Anti-Biofouling	4.62	30	*Adv. Sci.*, 2019, **6**, 1900547
11	POP-*o*NH_2-AO	POP	4.36	56	*Nat. Commun.*, 2018, ***9***, 1644
12	PAO hydrogel	Hydrogel	4.87	28	*Ind. Eng. Chem. Res.*,2015, **55**, 4103-4109

Star (*) represent the COF-SO_3H adsorbed uranium from concentrated seawater where uranium concentration is 10 ppb.

Table S14. Comparison of this work with other related investigations of enrichment index of uranium. $K_{(enrichment\ index)} = (U_{ads}/U_{aq})$; where U_{ads} (mg kg^{-1}) is the concentration of adsorbed uranium in the adsorbent and U_{aq} (mg kg^{-1}) is the final concentration of uranium in the natural seawater

Adsorbents	Uranium Uptake (mg/g)	Remaining Uranium Concentration Capacity (mg/g)	K (Enrichment Index)	Reference
i-MZIF90(50)	28.3	1.13	25044	This work
SSUP Fiber	12.33	2.67	4618	*Angew. Chem. Int. Ed.*, 2019, **58**, 11785
POP_1-AO	8.4	2.19	3836	*ACS Cent. Sci.*, 2021, **7**, 10, 1650–1656
UiO-66-3C4N	6.85	1.97	3477	*Angew. Chem. Int. Ed.*, 2020, **59**, 4262
PAF-CS	8.92	2.85	3130	*Chem. Sci.*, 2020, **11**, 1979
DNA-UEH	6.06	2.73	2220	*Nat. Commun.*, 2020, **11**, 5708
POP-*o*NH_2-AQ	4.36	2.15	2028	*Nat. Commun.*, 2018, **9**, 1644
MISS-PAF-1	5.79	2.87	2017	*ACS. Cent. Sci.*, 2019, **5**, 1432

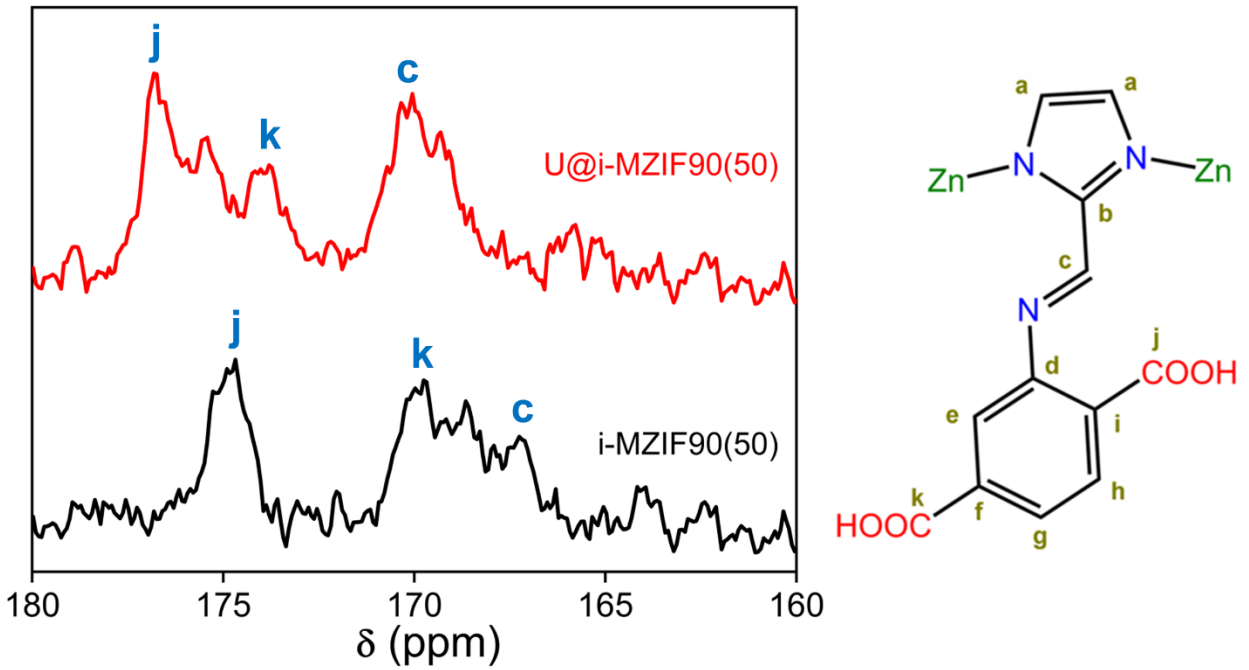

Fig. S33. ^{13}C solid state NMR spectra of i-MZIF90(50) before and after U extraction from water.

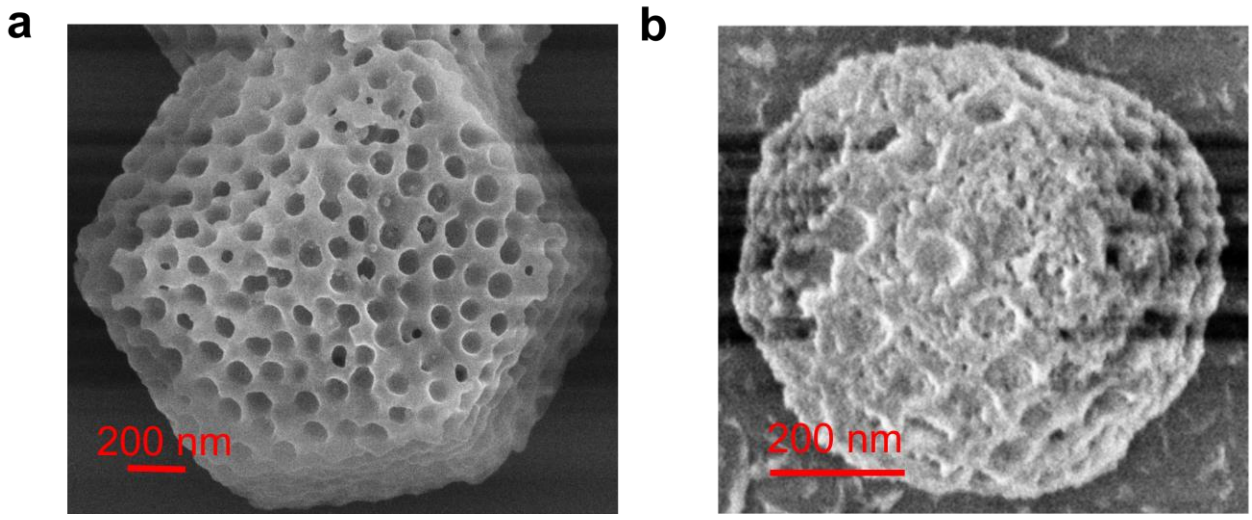

Fig. S34. a, and **b,** FESEM image before and after capture study for i-MZIF90(50).

Table S15. EDX analysis for U loaded ZIF-90.

Element	Weight%	Atomic%
C K	33.23	46.82
N K	20.97	25.33
O K	20.13	21.29
Zn L	25.19	6.52
U M	0.48	0.03
Totals	**100.00**	**100.00**

Table S16. EDX analysis for U loaded i-MZIF90(50).

Element	Weight%	Atomic%
C K	46.24	59.57
N K	13.32	14.71
O K	22.61	21.87
Zn L	15.65	3.70
U M	2.18	0.14
Totals	46.24	59.57

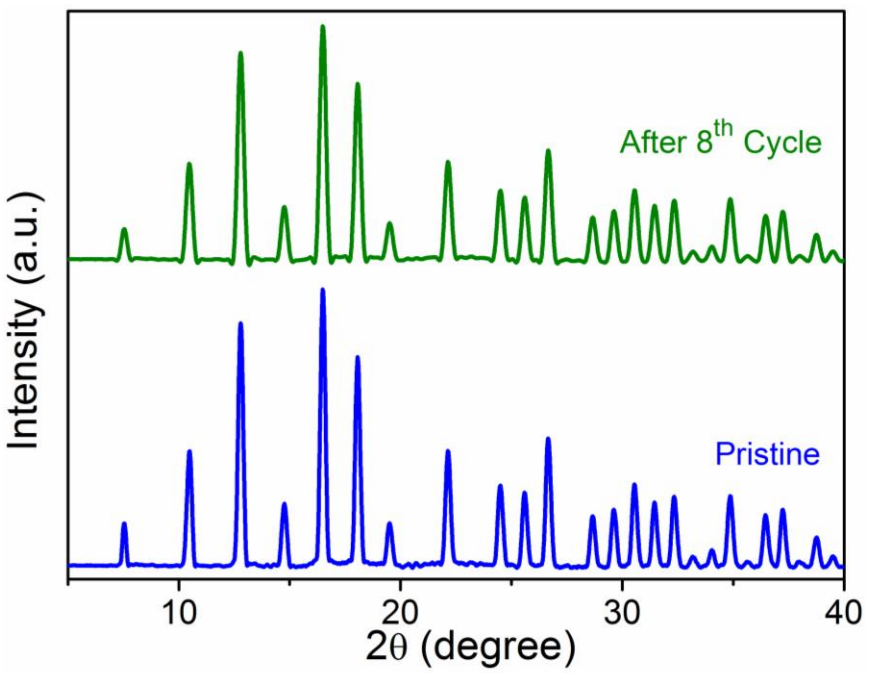

Fig. S35. PXRD patterns of i-MZIF90(50) before and after capture study in deionized water.

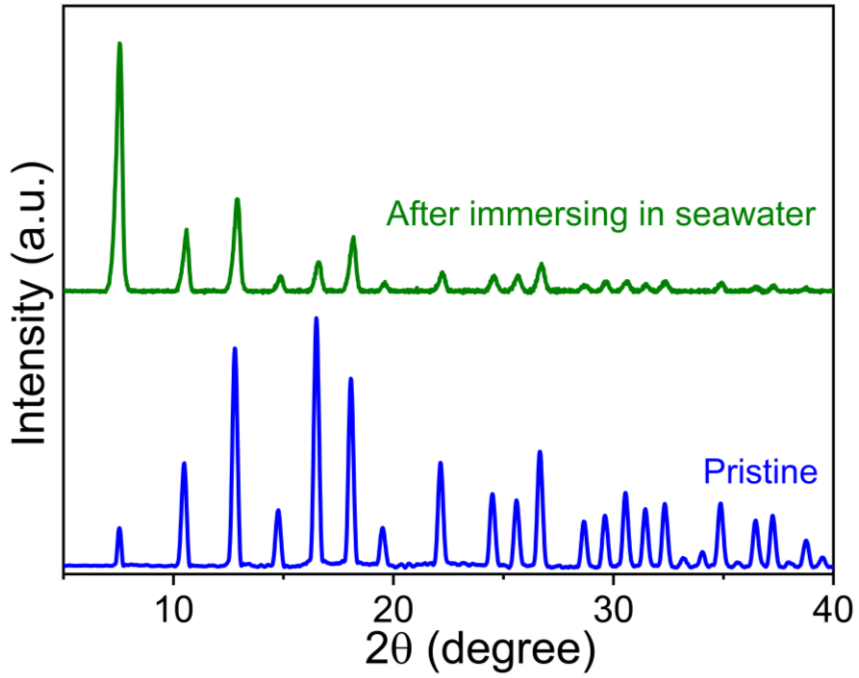

Fig. S36. PXRD patterns of pristine i-MZIF90(50) and after immersing in seawater for 25 days.

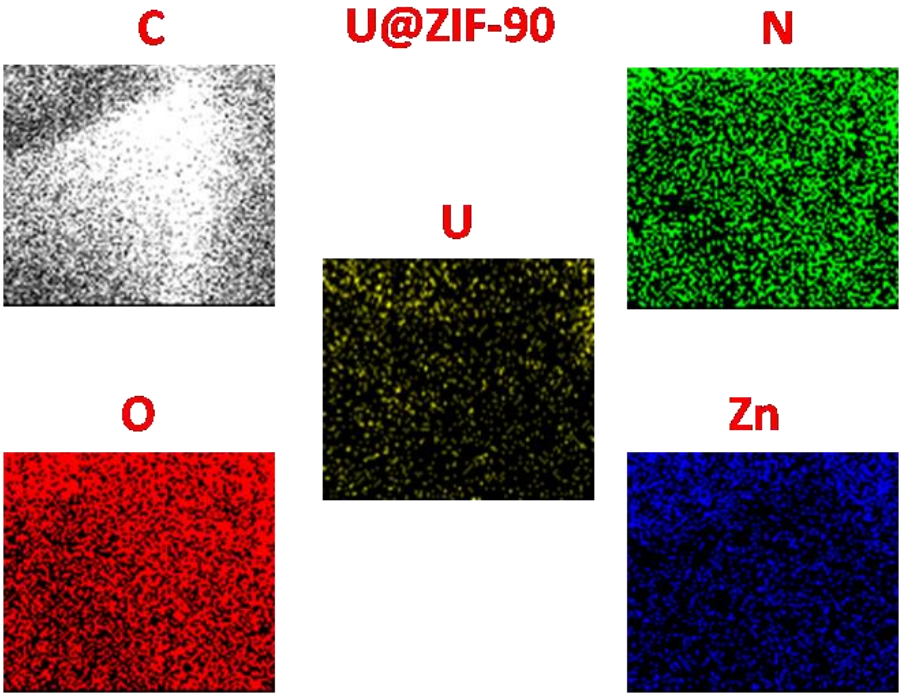

Fig. S37. Elemental mapping from FESEM experiment. The mapping shows successful loading of U in the ZIF-8.

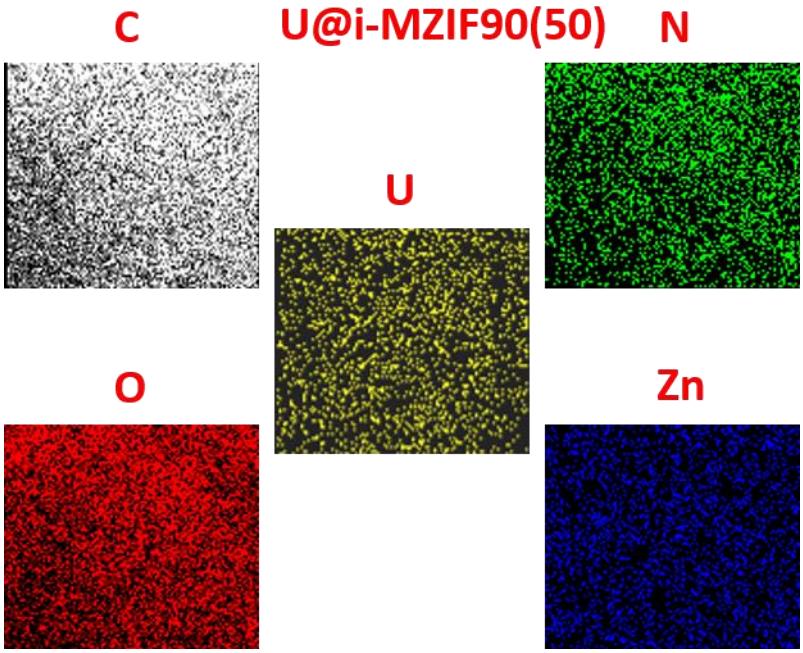

Fig. S38. Elemental mapping from FESEM experiment. The mapping shows successful loading of U in the i-MZIF90(50).

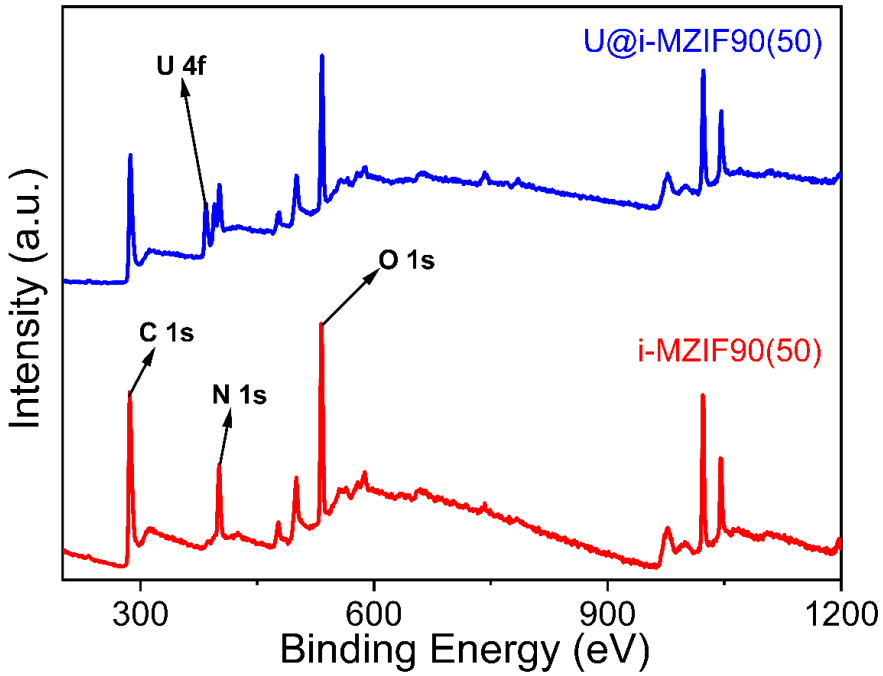

Fig. S39. XPS survey spectra of i-MZIF90(50) before and after U capture.

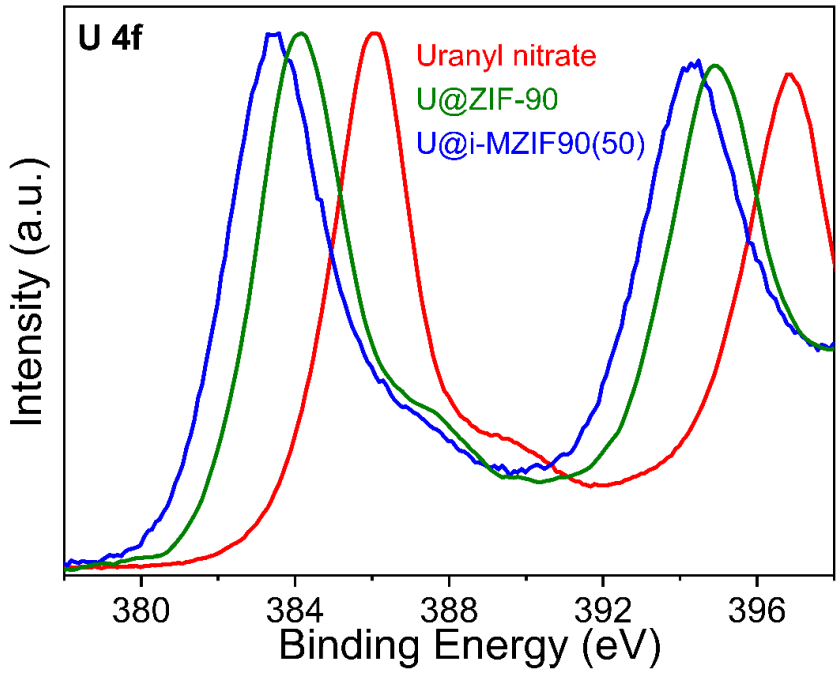

Fig. S40. High resolution XPS spectra of U 4f for Uranyl nitrate, U@ZIF-90 and i-MZIF90(50). The characteristics peaks for U 4f relatively shifted more lower binding energy after capture studied, indicates that U is more tightly bind with the i-MZIF90(50) compared to ZIF-90.

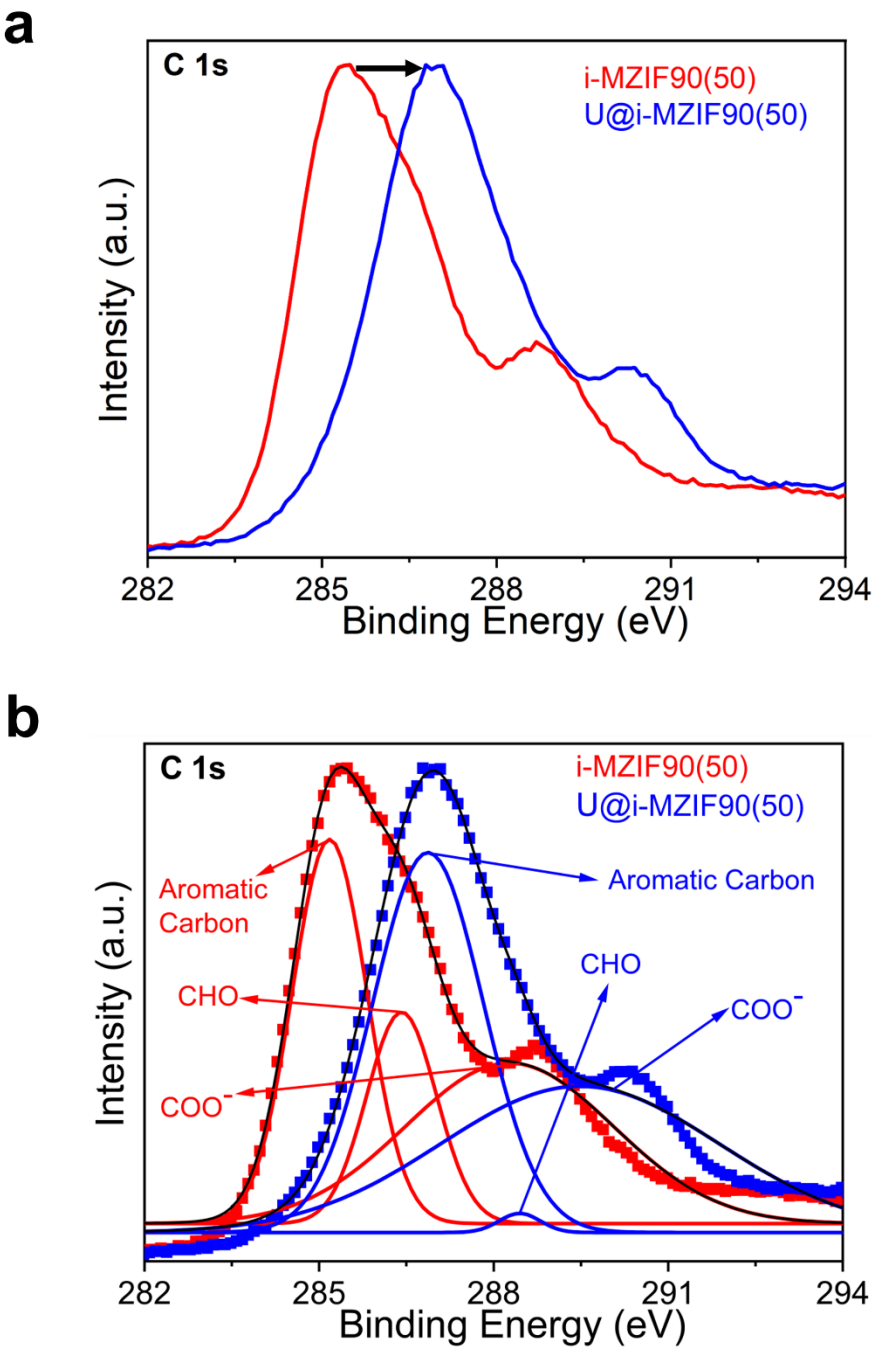

Fig. S41. High resolution C 1s XPS spectra of i-MZIF90(50) before and after capture of U. **a,** The characteristic peaks for C shifted to higher energy after loading of U in the framework indicates strong interaction with U and the framework. **b,** Deconvoluted peaks confirm U strongly interacted with the framework.

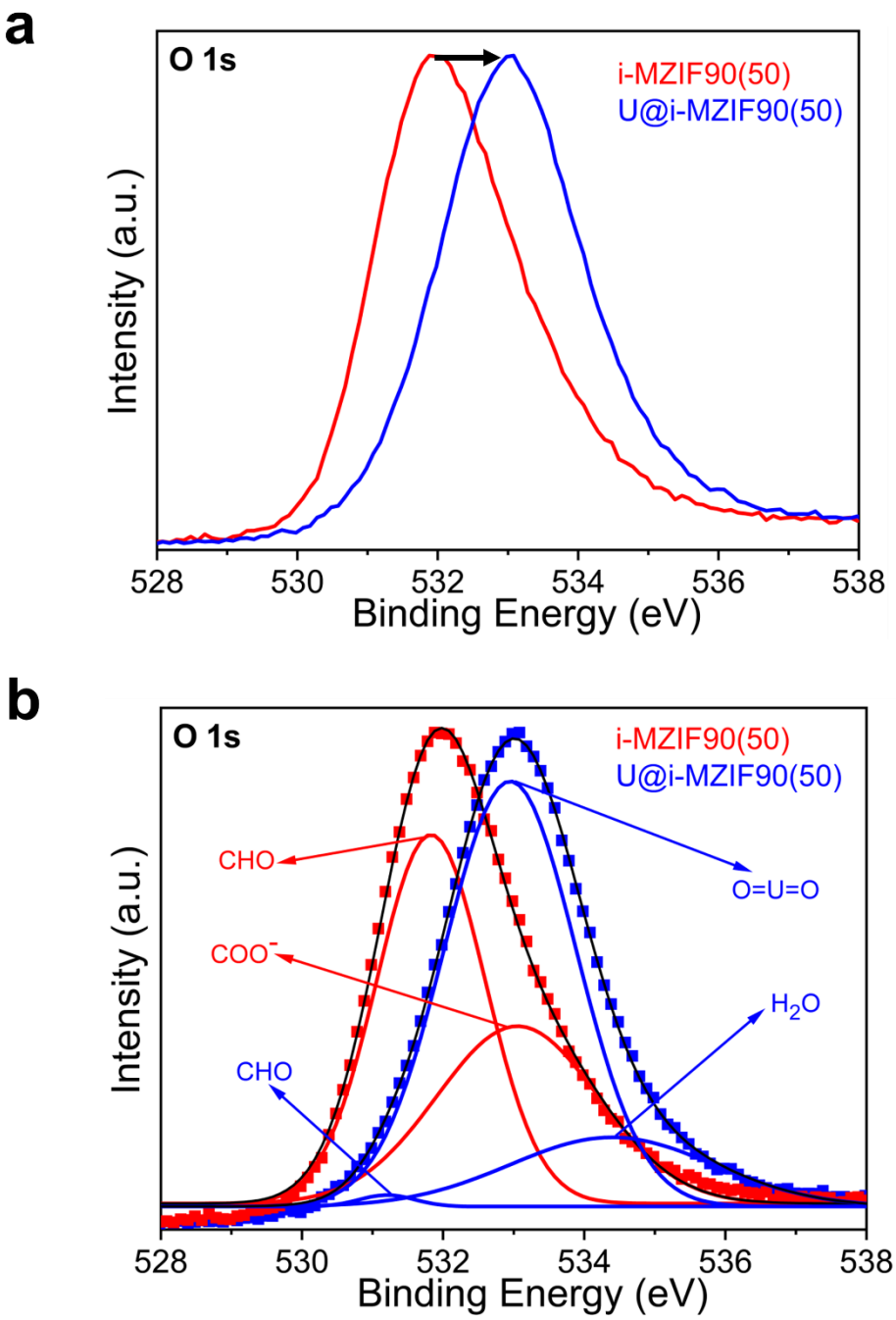

Fig. S42. High resolution XPS spectra of O 1s spectra of i-MZIF90(50) before and after capture of U. **a,** The characteristic peaks for O shifted to higher energy after loading of U in the framework indicates strong interaction with U and the framework. **b,** Deconvoluted peaks confirm U strongly interacted with the framework.

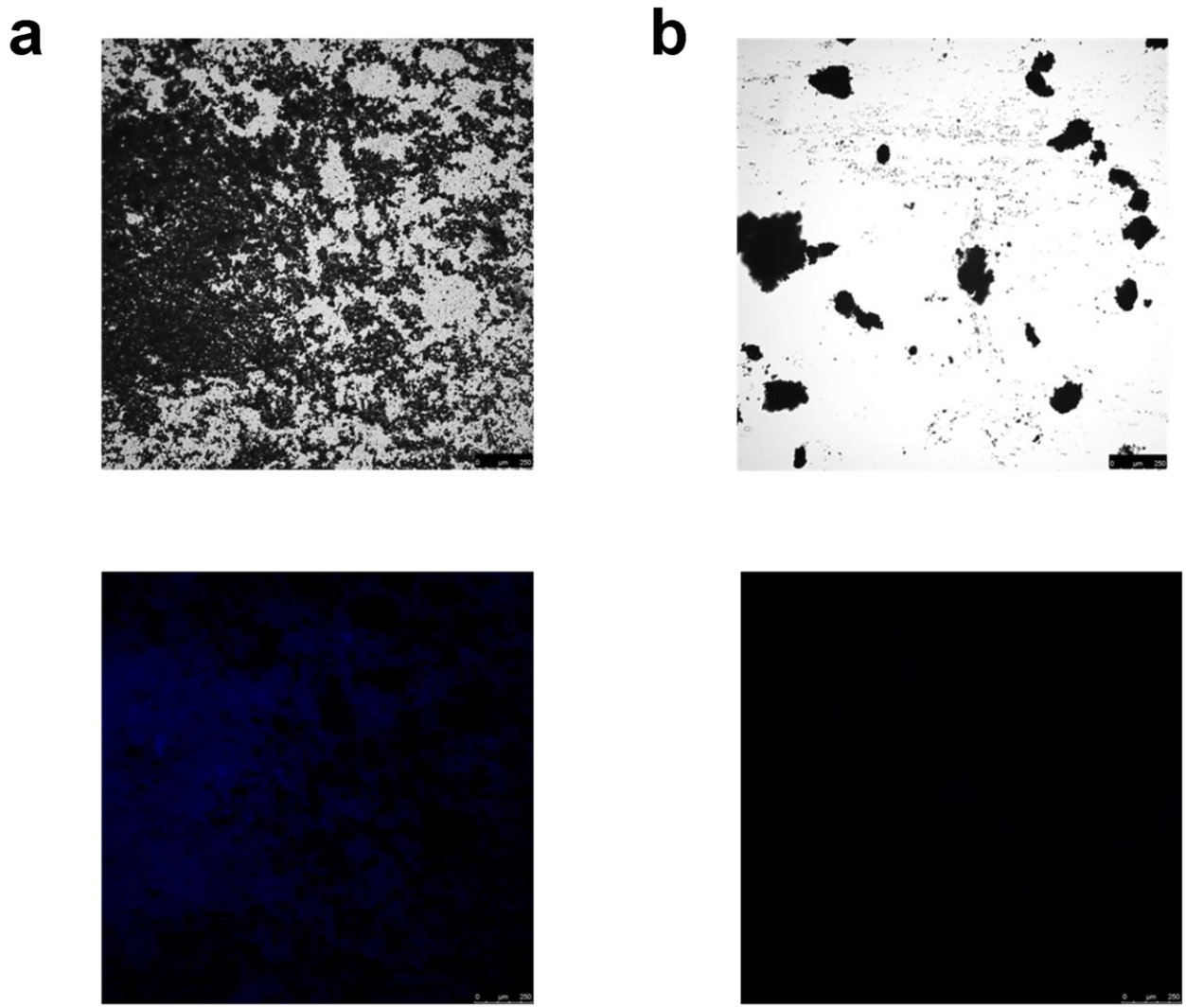

Fig. S43. a and **b,** Fluorescence imaging of i-MZIF90(50) before and after U capture studies.

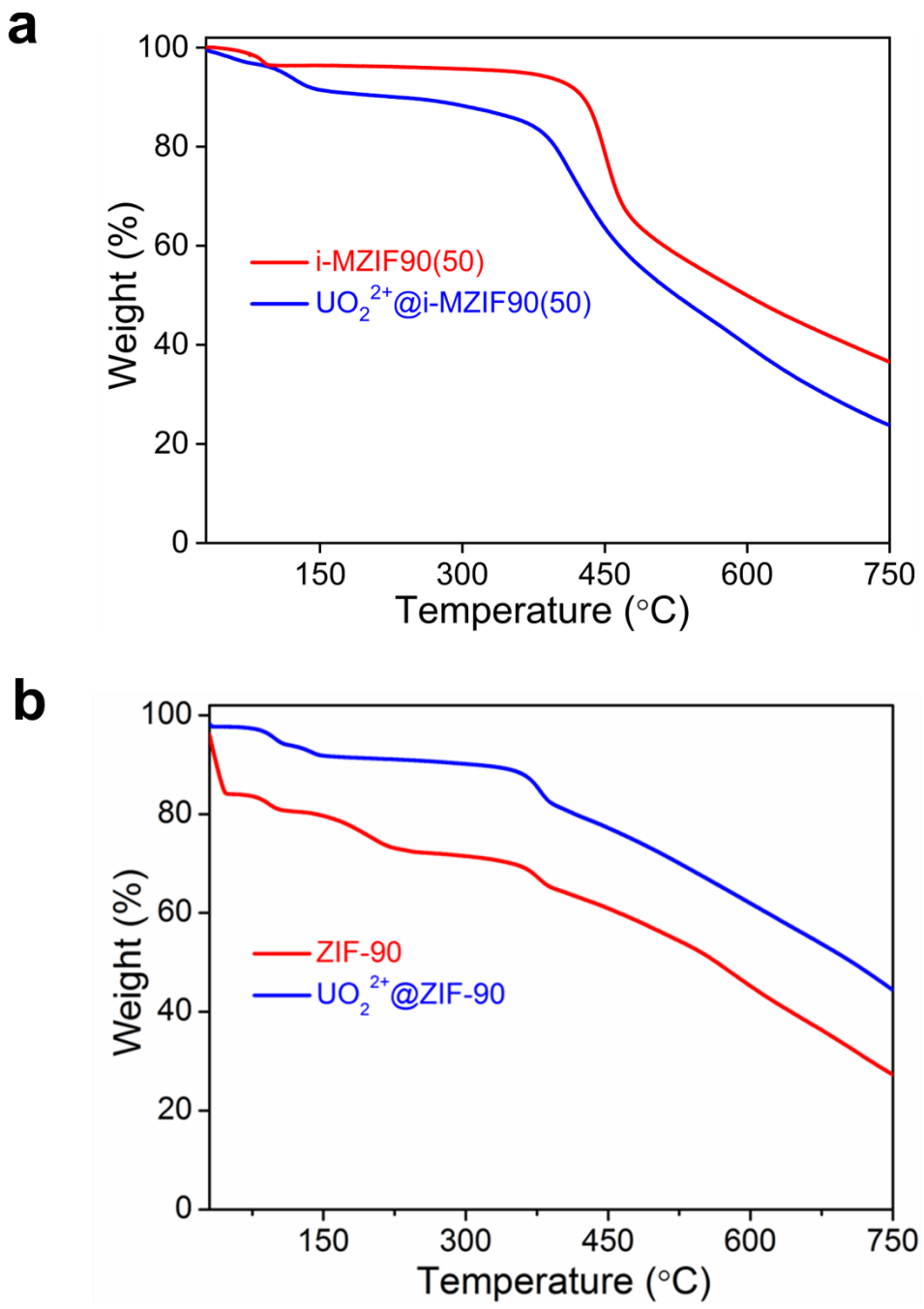

Fig. S44. TGA curves before and after capture studies. **a,** i-MZIF90(50); **b,** ZIF-90.

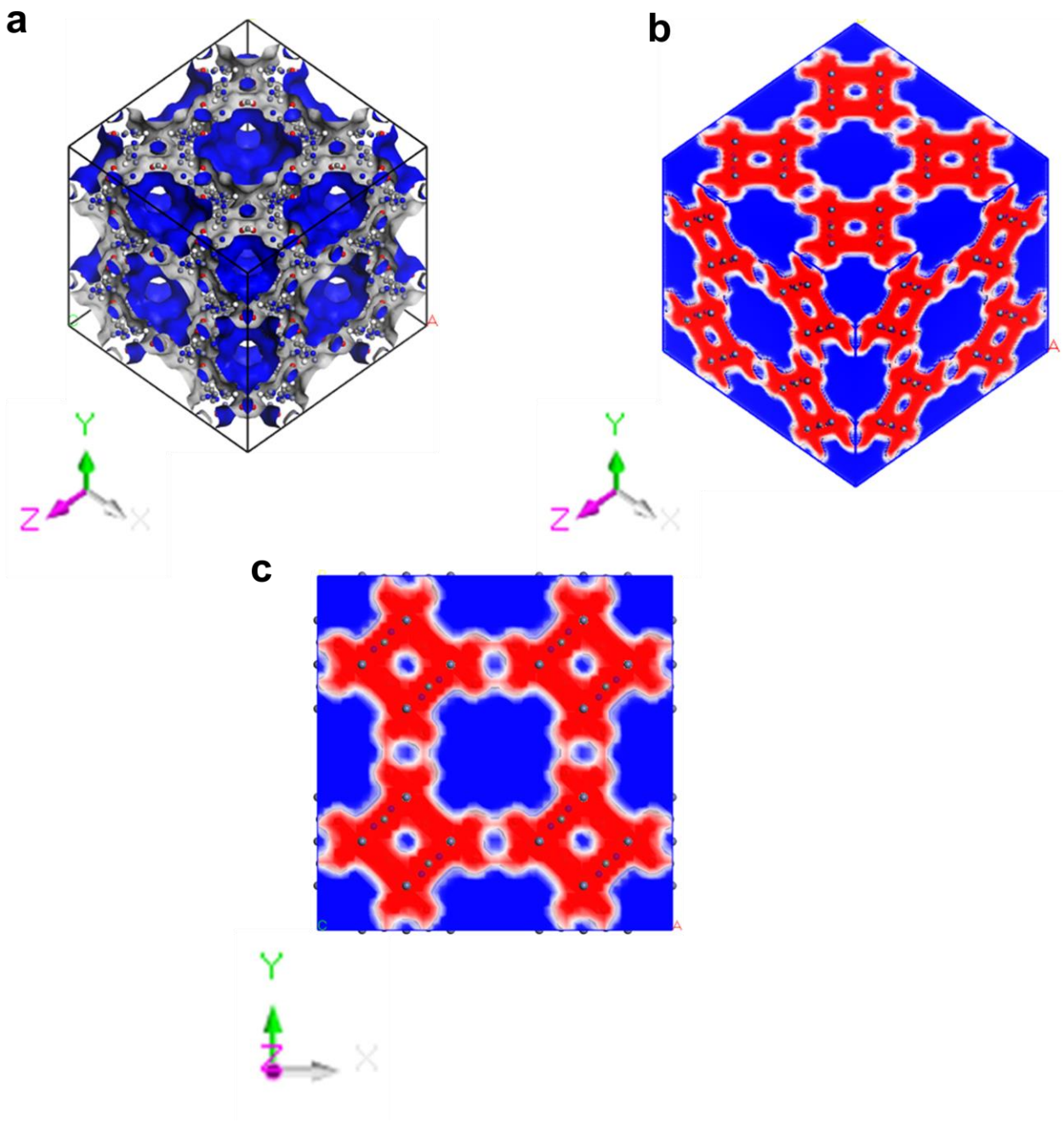

Fig. S45. **a,** 3D Cannoli surface of i-MZIF90(50), blue color shows the hollow pore of MOF. **b,** 3D cannoli surface with volume; blue color: pore volume, red color: packed region. **c,** one dimensional cannoli surface with volume derived from figure

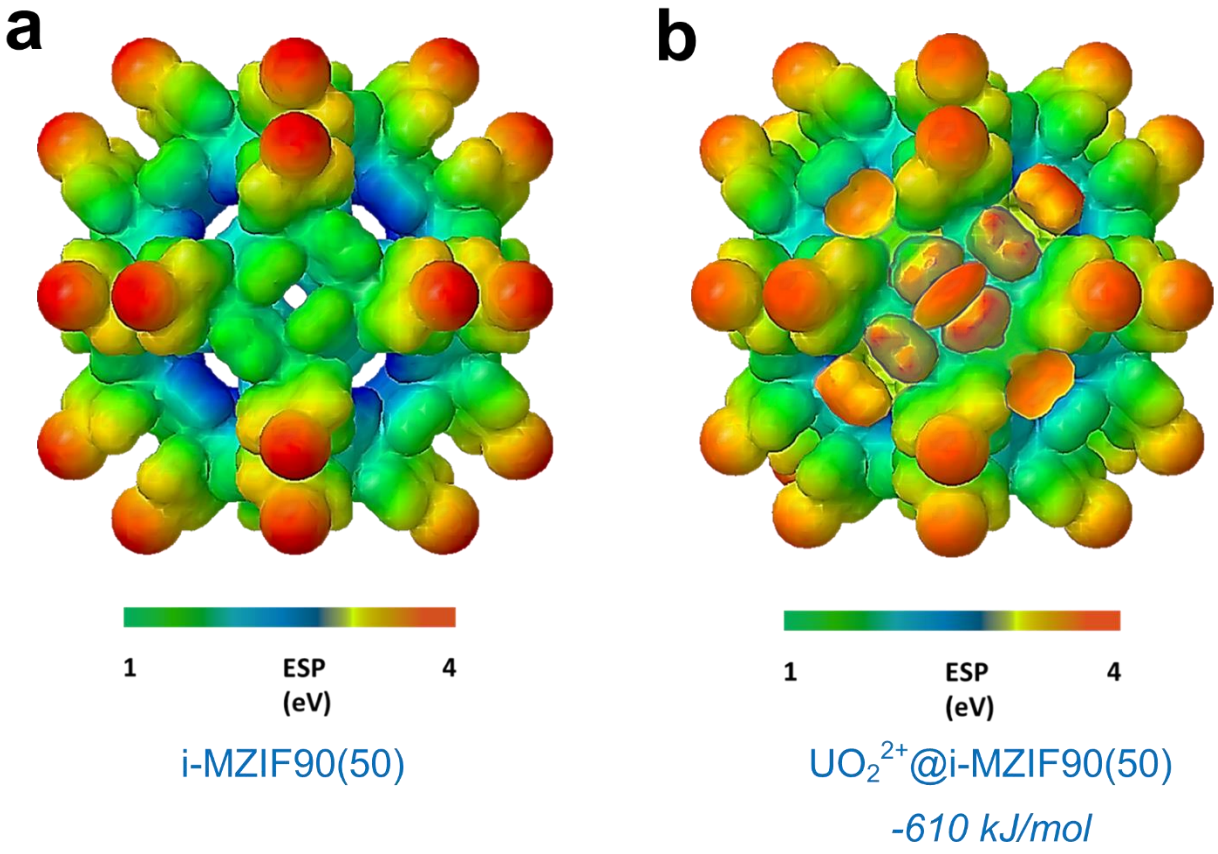

Fig. S46. **a,** ESP distribution of i-MZIF90(50) unit cell and **b,** ESP distribution in i-MZIF90(50) after UO_2^{2+} interactions. The ESP color scale in both the cases represent presence of low energy (green), medium energy (blue) and high energy (red) packets.

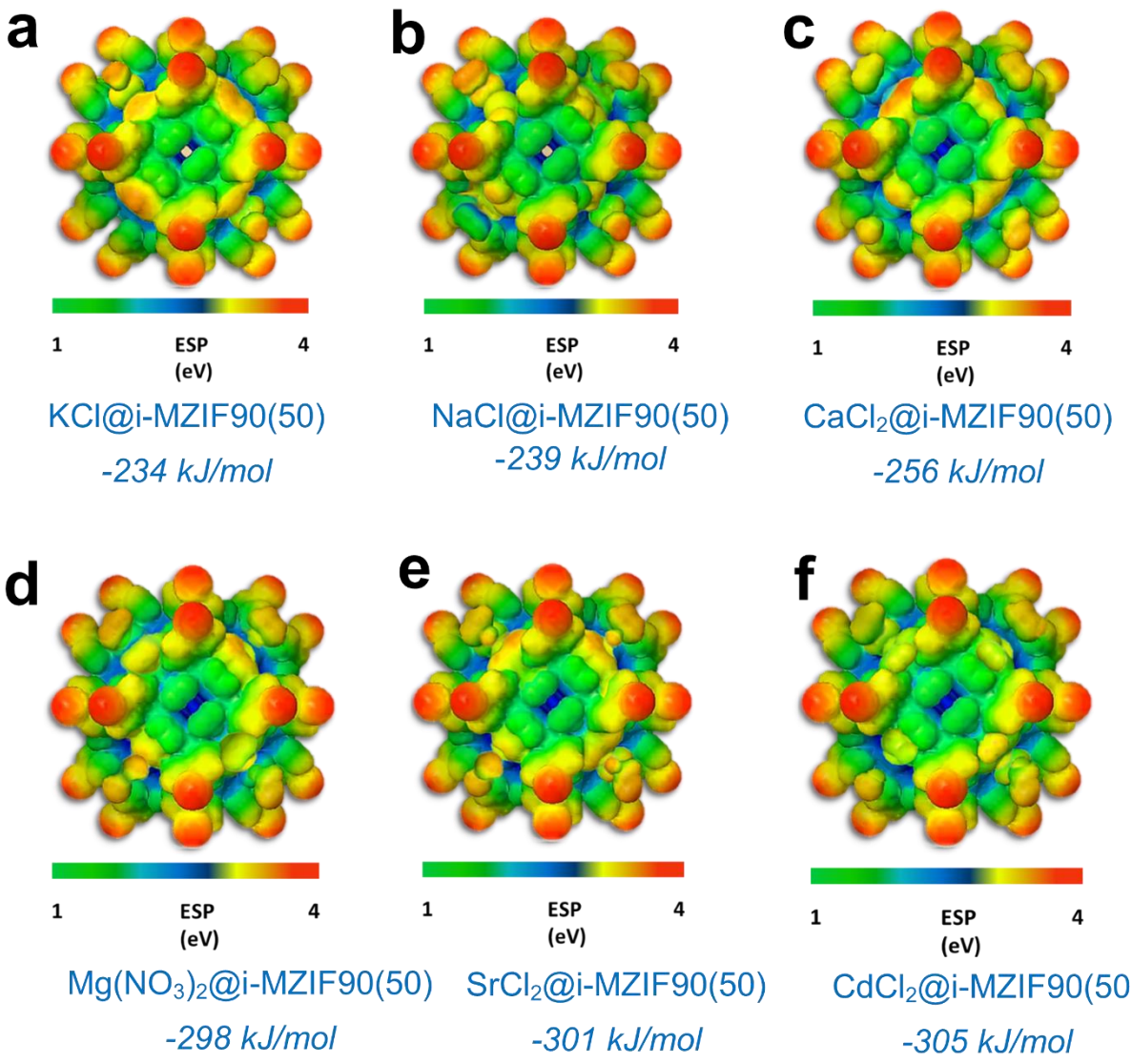

Fig. S47. ESP distribution of i-MZIF90(50) unit cell after interaction with various cations. **a,** KCl, **b,** NaCl, **c,** $CaCl_2$, **d,** $Mg(NO_3)_2$, **e,** $SrCl_2$, **f,** $CdCl_2$. The ESP color scale in both the cases represent presence of low energy (green), medium energy (blue) and high energy (red) packets.

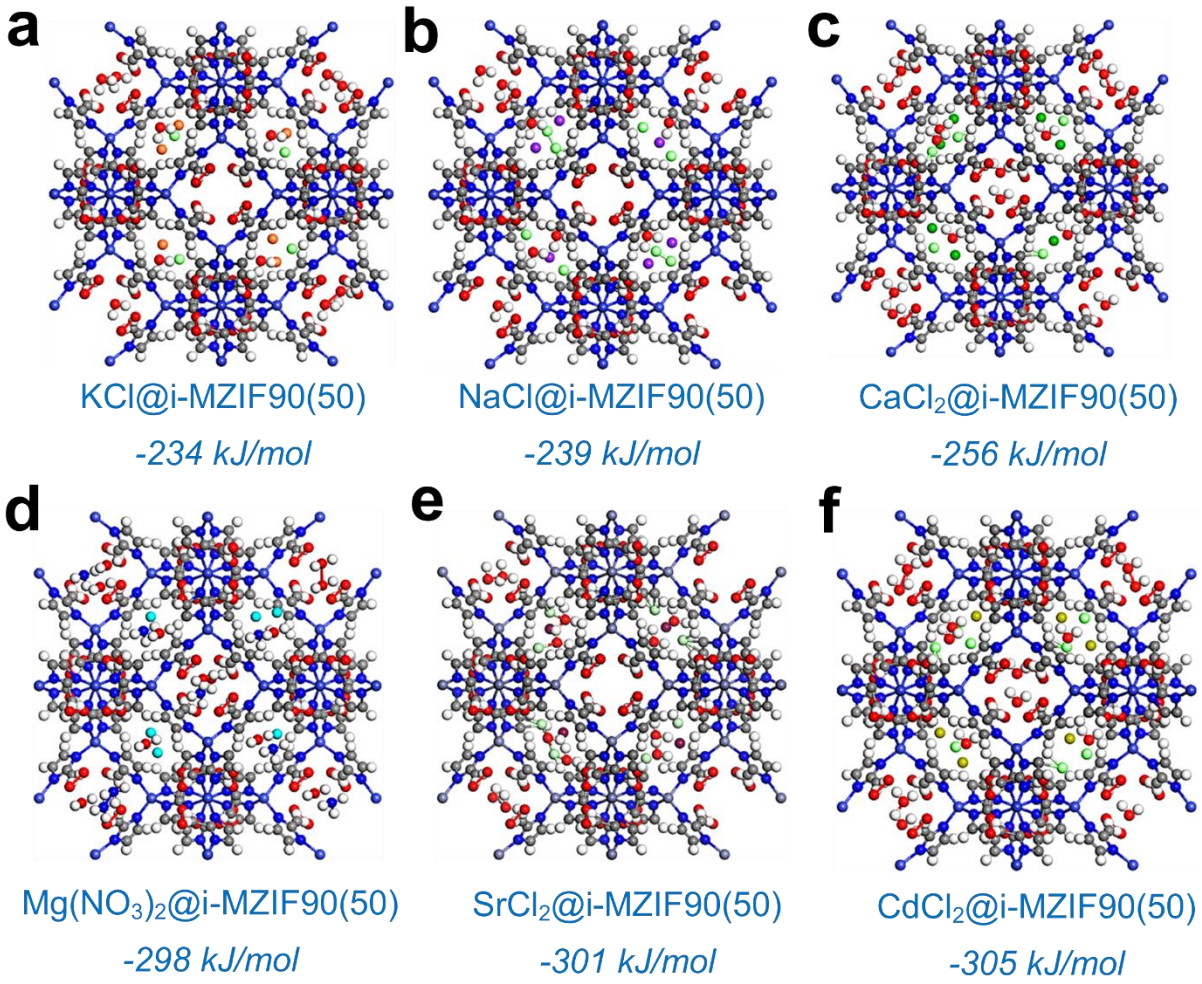

Fig. S48. Chemical structure of i-MZIF90(50) unit cell after interaction with various cations. **a,** KCl, **b,** NaCl, **c,** $CaCl_2$, **d,** $Mg(NO_3)_2$, **e,** $SrCl_2$, **f,** $CdCl_2$. Atom legend: K (Orange), Na (Purple), Ca (Olive Green), Mg (Cyan), Sr (Brown), Cd (Pale Yellow), Cl (Pale Green), N (Blue), O (Red), C (Gray) and H (White).

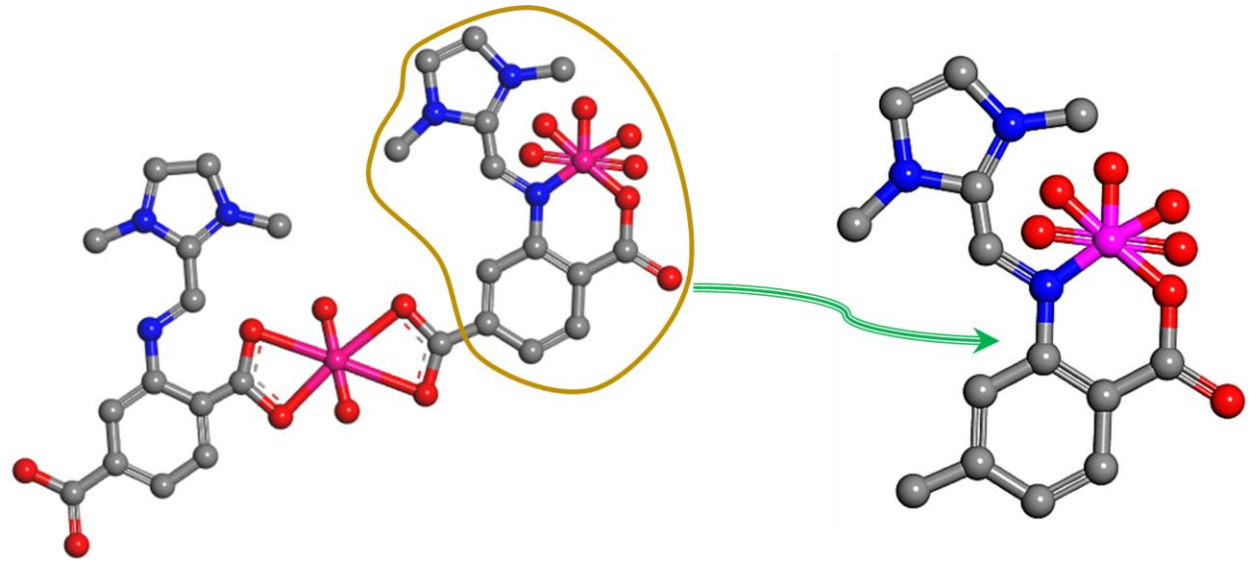

Fig. S49. Interaction sites of UO_2^{2+} in the i-MZIF90(50) Uranium atom is showed with Pink color. Atom color legend kept consistent with Fig. S48.

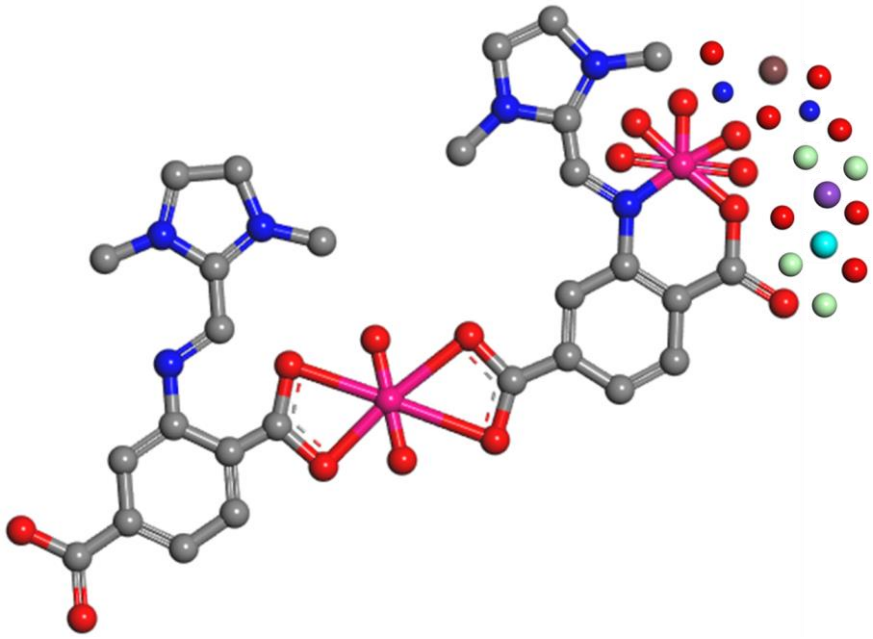

Fig. S50. Selective interaction of UO_2^{2+} with the i-MZIF90(50) presence of a wide range of interfering cations which are commonly found in natural seawater. Uranium atom is showed with Pink color. Atom color legend kept consistent with Fig. S48.

Movie S1. Movie showing breakthrough experiments, where 1.0 g ionic macroporous MOF (i-MZIF90(50)) was loaded in the column.

Reference

1. C. Liu, Q. Liu and A. Huang, *Chem. Commun.*, 2016, **52**, 3400.

2. Y. Yang, J. Cheng, B. Wang, Y. Guo, X. Dong and J. Zhao, *Microchim. Acta*, 2019, **186**, 101.

3. Y. Yuan, Q. Meng, M. Faheem, Y. Yang, Z. Li, Z. Wang, D. Deng, F. Sun, H. He, Y. Huang, H. Sha and G. Zhu, *ACS Cent. Sci.*, 2019, **5**, 1432.